

## PDF hosted at the Radboud Repository of the Radboud University Nijmegen

The following full text is a preprint version which may differ from the publisher's version.

For additional information about this publication click this link.

<http://hdl.handle.net/2066/143907>

Please be advised that this information was generated on 2021-04-16 and may be subject to change.

# RG flows of Quantum Einstein Gravity in the linear-geometric approximation

Maximilian Demmel<sup>a</sup>, Frank Saueressig<sup>b</sup>, Omar Zanusso<sup>c</sup>

<sup>a</sup> *PRISMA Cluster of Excellence & Institute of Physics (THEP),  
University of Mainz, Staudingerweg 7, D-55099 Mainz, Germany*

<sup>b</sup> *Institute for Mathematics, Astrophysics and Particle Physics (IMAPP),  
Radboud University Nijmegen, Heyendaalseweg 135, 6525 AJ Nijmegen, The Netherlands*

<sup>c</sup> *Theoretisch-Physikalisches Institut, Friedrich-Schiller-Universität Jena,  
Max-Wien-Platz 1, 07743 Jena, Germany*

---

## Abstract

We construct a novel Wetterich-type functional renormalization group equation for gravity which encodes the gravitational degrees of freedom in terms of gauge-invariant fluctuation fields. Applying a linear-geometric approximation the structure of the new flow equation is considerably simpler than the standard Quantum Einstein Gravity construction since only transverse-traceless and trace part of the metric fluctuations propagate in loops. The geometric flow reproduces the phase-diagram of the Einstein-Hilbert truncation including the non-Gaussian fixed point essential for Asymptotic Safety. Extending the analysis to the polynomial  $f(R)$ -approximation establishes that this fixed point comes with similar properties as the one found in metric Quantum Einstein Gravity; in particular it possesses three UV-relevant directions and is stable with respect to deformations of the regulator functions by endomorphisms.

*Keywords:* Quantum Gravity, Asymptotic Safety, Functional Renormalization Group

---

## 1. Introduction

### 1.1. Asymptotic safety: a primer

Asymptotic Safety [1, 2, 3] provides a natural mechanism to define a consistent and predictive quantum theory of gravity within the framework of quantum field theory [4, 5, 6, 7]. The proposal is conservative in the sense that the gravitational degrees of freedom are carried by the space-time metric and invariance under coordinate transformations is retained as

---

*Email addresses:* demmel@thep.physik.uni-mainz.de (Maximilian Demmel), f.saueressig@science.ru.nl (Frank Saueressig), omar.zanusso@uni-jena.de (Omar Zanusso)

a symmetry principle. The essence of the construction is a non-Gaussian fixed point (NGFP) of the gravitational renormalization group (RG) flow, which controls the gravitational interactions at high energies. Ideally, this NGFP should come with a finite number of relevant directions in order to ensure predictivity of the construction. RG trajectories which are dragged into the NGFP possess a well-defined UV limit since the dimensionless couplings remain finite and scattering amplitudes are save from unphysical UV divergences.

Initially proposed by Weinberg, the systematic investigation of Asymptotic Safety started with the advent of the functional renormalization group equation (FRGE) for the gravitational effective average action  $\Gamma_k$  [8]

$$\partial_t \Gamma_k[\Phi, \bar{\Phi}] = \frac{1}{2} \text{STr} \left[ \left( \Gamma_k^{(2)} + \mathcal{R}_k \right)^{-1} \partial_t \mathcal{R}_k \right]. \quad (1)$$

Here  $t \equiv \ln k/k_0$  is the “renormalization group time” and  $\mathcal{R}_k$  constitutes an IR regulator, which acts as a mass term for quantum fluctuations of the gravitational field with momenta  $p^2 \lesssim k^2$ . The Hessian  $\Gamma_k^{(2)}$  denotes the second variation of  $\Gamma_k$  with respect to the fluctuation fields  $\Phi$  at fixed background fields  $\bar{\Phi}$  and is thus a matrix valued inverse propagator in field space. The trace  $\text{STr}$  contains a sum over loop momenta  $p^2$  and internal indices. The regulator dependence in (1) ensures that the integration over momenta is UV- and IR-finite and “peaked” at momenta  $p^2 \approx k^2$ . Thus the flow of  $\Gamma_k$  is driven by quantum fluctuations at the scale  $k^2$  and realizes the successive integrating out of field modes “shell-by-shell” in momentum space as  $k$  is lowered. In fact, taking the limit  $k \rightarrow 0$  all quantum fluctuations are integrated out and  $\lim_{k \rightarrow 0} \Gamma_k = \Gamma_0$  coincides with the effective action of the theory.

Formally, the FRGE is an exact equation carrying the same information content as the path integral from which it is derived in [9] and independently in [10]. Moreover, constructing complete solutions  $\Gamma_k$  for  $k \in [0, \infty[$  is actually equivalent to solving the underlying path integral or, in other words, to the renormalization of the theory [11, 12]. A particular strength of (1) is that it allows to compute approximate solutions for the gravitational RG flow without resorting to an expansion in a small parameter or presupposing the renormalizability of the theory. Performing a derivative expansion or vertex expansion of  $\Gamma_k$  yields approximate RG flows which are non-perturbative in nature and whose range of validity extends far beyond the Gaussian regime of perturbation theory. These techniques have played an essential role in establishing confidence in the Asymptotic Safety conjecture.

The first set of evidence supporting the Asymptotic Safety scenario comes from projecting the RG flow entailed by (1) to a finite number of coupling constants, restricting the operators contained in  $\Gamma_k$  to a finite subset.

Starting from the seminal works which projected the gravitational effective average action onto the operators included in the Einstein-Hilbert action [8, 13, 14], the gravitational RG flow has been successively projected onto operator subspaces of increasing complexity and field content. The existence of a NGFP has then been clearly established in the Einstein-Hilbert truncation [15, 16, 17, 18] and its extensions including the square of the scalar curvature  $R^2$  [19, 20, 21],  $f(R)$ -type polynomial truncations where the effective average action is approximated by polynomials of the scalar curvature [22, 23, 24, 25, 27, 26], the square of the Weyl tensor [28, 29], the Gibbon-Hawking-York boundary terms relevant for black holes physics [30], and in truncations where the quantum effects of the ghost sector are taken into account [31, 32, 33].

In particular the polynomial  $f(R)$ -truncations [22, 23, 24, 25, 26, 27] provide an important indication for the predictivity of Asymptotic Safety: including curvature terms  $R^N$  for  $N \geq 3$  in the polynomial ansatz does not unveil new, relevant directions and the number of relevant parameters remains three. In fact, even the initial systematic studies [20, 22, 23] already indicated that the irrelevance of the new directions, as measured by the critical exponents, increases with the order of the polynomial expansion suggesting that power counting might still constitute a good ordering principle at the NGFP. More formal arguments supporting the predictivity of the NGFP have been advocated in [34].

In contrast to perturbation theory, the FRGE allows to test Asymptotic Safety for various spacetime dimensions and, in particular, away from both the upper and lower critical dimensions of gravity. In fact the dimension of spacetime can be treated as parameter: the existence of a NGFP can thus be shown for any dimension greater than two [16, 35, 36] and it is easily seen that the NGFP of Asymptotic Safety merges with the Gaussian fixed point at the lower critical dimension  $d = 2$ . Thus Asymptotic Safety is the simplest and most effective generalization of Asymptotic Freedom. Finally, the properties of the NGFP seem to be mostly determined by the integration of the “trace-type” degrees of freedom of the metric, which are readily visible in the so-called conformally reduced approximation [37, 38, 39, 40, 41]. In fact, a recent interpretation by ’t Hooft [42] advocates the viewpoint that the conformal degrees of freedom of the metric should be integrated out first, leaving an effective field theory for the conformal sector.

More advanced evidence for Asymptotic Safety comes from studying expectation values of the fluctuation field (so-called “bi-metric” truncations), signature-dependent effects and anisotropic scaling effects. Bi-metric truncations explicitly take into account the dependence of  $\Gamma_k$  on the fluctuation fields and are natural generalizations of the aforementioned “single-metric” truncations that provide the first body of evidence. This program has been initiated in [43, 44] and turns out to be crucial for understanding the background covariance of Asymptotic Safety [45, 46], precision compu-

tations elucidating the structure of the NGFP [47, 48, 49] and establishing monotonicity properties of the gravitational RG flow expected from standard RG arguments [50]. The dependence of the NGFP on the signature of the metric was first investigated in [51], showing that the Asymptotic Safety mechanism is realized independently of the signature of the metric [52]. Asymptotic Safety has also been showed to play a significant role in understanding of the phase diagram of the anisotropic theories of gravity, dubbed Hořava-Lifshitz gravity [53]. Hořava-Lifshitz gravity is conjectured to be perturbatively renormalizable and the fixed point structure underlying this conjecture as well as its relation to the Asymptotic Safety proposal has recently been clarified [54].

Progress has also been made in achieving a deeper mathematical and physical understanding of the Asymptotic Safety mechanism. On the one hand, a computer based algorithm for evaluating the derivative expansion of the gravitational FRGE was proposed in [55] and further developed in [56, 57], showing that the expansion is “computable” to any order in a strict mathematical sense. On the other hand, a physical explanation for Asymptotic Safety based on paramagnetic dominance has been advocated in [58] which draws a clear and intriguing analogy with the pictorial representation of Asymptotic Freedom in which charges are screened by virtual pair production.

Paralleling the development of the Asymptotic Safety program based on the FRGE, similarly encouraging results have been obtained from Monte Carlo simulations using dynamical triangulations methods [62]. In this case, macroscopic spacetimes are glued together from piecewise linear building blocks (simplices) and the statistical weight of a configuration is given by the discretized gravitational action. A particularly successful implementation of this idea are Causal Dynamical Triangulations (CDT) [63], reviewed in [64], which imprint a causal structure on the triangulations. Most impressively, the CDT program has established the existence of a “classical phase” where the large-scale properties of the triangulated geometries resemble those observed in the real world [65, 66]. Moreover, there is evidence for a second-order phase transition line which may allow to take the continuum limit of the underlying lattice theory in a controlled way [67, 68, 69]. From a RG perspective, the second-order phase transition may represent the NGFP found by continuum methods, thereby linking CDT and the Asymptotic Safety conjecture, also see [70, 71] for a more detailed discussion of this point.

Based on these findings, the Asymptotic Safety scenario in which gravitational degrees of freedom are captured by fluctuations of the spacetime metric is on firm grounds. This raises the interesting question whether formulating the theory in terms of metric fluctuations is the only possibility to achieve Asymptotic Safety. At the classical level, there are indeed many formulations (metric, first-order formalism, etc.) which give rise to the same

dynamics.<sup>1</sup> It is far from clear, however, that this also holds at the level of the quantum theory. This question is closely related to the construction of the measure of the gravitational path integral which can crucially influence the content of FRGE. While the FRGE retains its structural form,  $\text{Str}$  and  $\Gamma_k^{(2)}$  may acquire different meanings if the derivation of the FRGE is not based on a field-reparametrization invariant formulation of the path-integral.

### 1.2. Scope of the present work

The goal of this paper is the construction of a novel, geometric FRGE based on gauge-invariant fluctuation fields and a specific choice of path-integral measure which are adapted to the fiber-bundle structure of the gravitational configuration space. The structure of the resulting geometric FRGE is significantly simpler than the one underlying non-geometric constructions, since it does not contain contributions from the gauge-fixing, ghost sector and auxiliary traces encoding the Jacobians originating from the transverse-traceless decomposition [72] of the fluctuation field. In this sense our construction is more economic than earlier versions of the FRGE based on the Vilkovisky-De Witt formalism [73, 74, 18] and avoids the complications associated with evaluating the flow on-shell [75]. In the concrete computations based on the geometric flow equation we truncate the map between the metric fluctuations and gauge-invariant fields at the linear order. This linear-geometric approximation can also be obtained from non-geometric flow equations for a specific choice of gauge-fixing and regulator. Geometrically, this corresponds to an approximation where the Vilkovisky connection on the gauge-bundle is neglected.

In order to get a first impression of the RG flow encoded in the geometric FRGE, we derive the beta functions of the Einstein-Hilbert and  $f(R)$ -truncation including non-trivial endomorphisms in the coarse-graining operator. Based on these beta functions, we identify a NGFP whose properties are remarkably similar to the ones found in non-geometric computations. In particular, it also comes with three relevant directions and the stability coefficients are in good agreement with the ones found in previous studies. Our results exhibit only a very mild dependence on the regularization scheme which is mitigated even further when considering observables such as the critical exponents of the NGFP. Finally, we exploit the freedom in selecting the coarse-graining scheme and apply the principle of minimum sensitivity (PMS) [76, 77] in order to optimize the physics content of the computation by minimizing the scheme-dependence of the observables. Notably, imposing the PMS conditions significantly improves the convergence of the fixed point properties within the series of polynomial truncations.

---

<sup>1</sup>For first studies of the gravitational RG flows employing vielbein-connection variables and the ADM formalism, see [59, 60] and [61], respectively.

As it will turn out [78], the field parametrization invariant formulation of the FRGE is closely related to another key challenge currently faced by the Asymptotic Safety program, the extension of the finite-dimensional truncations discussed above to an infinite set of couplings. The latter are implemented by approximating  $\Gamma_k$  by scale-dependent functions. Substituting such an ansatz into (1) then yields a non-linear partial differential equation (PDE) which governs the  $k$ -dependence of the function contained in the ansatz and the fixed points discussed above are promoted to  $k$ -stationary, global solutions of this PDE. The simplest ansatz of this type approximates the gravitational part of  $\Gamma_k$  by a function of the scalar curvature  $R$

$$\Gamma_k^{\text{grav}}[g] = \int d^d x \sqrt{g} f_k(R). \quad (2)$$

This type of functional truncations has been considered in both three [79, 80, 81] and four dimensions [82, 83]. The three-dimensional studies demonstrated that the NGFP can consistently be promoted to a fixed function, and proved, for the first time, that this fixed function admits only a finite number of relevant deformations. The analogous construction in  $d = 4$  [84, 85] has proven to be highly non-trivial, however, and no satisfying fixed function has been found to date.

The remaining parts of the work are organized as follows. Sect. 2 contains the derivation of the geometric flow equation, discusses its connection to the non-geometric formulations, and outlines the approximations required for doing practical computations. As a first application, the Einstein-Hilbert truncation in the linear-geometric approximation is investigated in Sect. 3. In Sect. 4 we derive a new partial differential equation (PDE) governing the scale-dependence of  $f(R)$ -gravity including non-trivial endomorphisms in the coarse-graining scheme. The fixed point structure entailed by this PDE is analyzed in Sect. 5 and we conclude with a brief summary and outlook in Sect. 6. The technical tools needed for the construction of the beta functions are summarized in Appendix A.

## 2. Flow equation for gauge invariant fields

In this section we construct a Wetterich-type functional renormalization group equation for the gravitational effective average action [8], whose flow is solely driven by gauge invariant fields. The resulting FRGE is independent of the choice of gauge-fixing, because it invokes a precise cancellation among the un-physical polarization of the metric fluctuations  $h_{\mu\nu}$  and the ghost fields themselves. This leads to significant simplifications of (1) as compared to the past implementations that appeared in the literature, since the flow does not receive contributions from either ghost or gauge degrees of freedom, nor from the auxiliary fields that are usually considered to handle the transverse-traceless decomposition of  $h_{\mu\nu}$ .

### 2.1. The flow equation of metric QEG

The ultimate goal of Quantum Einstein Gravity is to give meaning to a path integral over “all” metrics  $\gamma_{\mu\nu}$  suitably weighted by a bare action  $S[\gamma_{\mu\nu}]$ . The bare action is invariant under the general coordinate transformations

$$\delta\gamma_{\mu\nu} = \mathcal{L}_v\gamma_{\mu\nu} \equiv v^\alpha \partial_\alpha \gamma_{\mu\nu} + \gamma_{\alpha\nu} \partial_\mu v^\alpha + \gamma_{\mu\alpha} \partial_\nu v^\alpha, \quad (3)$$

which have thus to be suitably factored out from the path integral of the effective action. Instead of studying the underlying path integral directly, in the Asymptotic Safety program one mainly utilizes an effective average action which interpolates smoothly between a UV bare action and the full effective action in the IR. The renormalization group flow of the effective average action is then governed by a functional RG equation (1) which can thus be directly used to investigate the theory’s properties. Our construction of the gravitational FRGE is based on the background field method. In this setting, one splits the quantum metric  $\gamma_{\mu\nu}$  into a fixed (though arbitrary) background metric  $\bar{g}_{\mu\nu}$  and corresponding fluctuations  $\hat{h}_{\mu\nu}$

$$\gamma_{\mu\nu} = \bar{g}_{\mu\nu} + \hat{h}_{\mu\nu}. \quad (4)$$

The background field formalism then allows to implement a symmetry transformation of the type (3) in two different ways. The gauge transformations generalizing (3) which need to be gauge-fixed are the quantum gauge transformations

$$\delta_Q \hat{h}_{\mu\nu} = \mathcal{L}_v \hat{h}_{\mu\nu}, \quad \delta_Q \bar{g}_{\mu\nu} = 0, \quad (5)$$

which are constructed such that the background metric is left invariant and only the fluctuations transform. However, a very important feature of the background field method is that it is always possible to explicitly maintain the so-called background gauge transformations

$$\delta_B \hat{h}_{\mu\nu} = \mathcal{L}_v \hat{h}_{\mu\nu}, \quad \delta_B \bar{g}_{\mu\nu} = \mathcal{L}_v \bar{g}_{\mu\nu}, \quad (6)$$

where the background metric is subject to a background coordinate transformation analogous to (3) and every other field, in particular  $h_{\mu\nu}$ , transforms as a tensor of its corresponding rank.

The fluctuation field is the natural variable of integration in the scale-dependent functional integral

$$\mathcal{Z}_k \equiv \int \mathcal{D}\hat{h}_{\mu\nu} \mathcal{D}C^\mu \mathcal{D}\bar{C}_\mu \exp \left\{ -\tilde{S}[\hat{h}, C, \bar{C}; \bar{g}] - \Delta_k S[\hat{h}, C, \bar{C}; \bar{g}] - S_{\text{source}} \right\}, \quad (7)$$

with  $\tilde{S}[\hat{h}, C, \bar{C}; \bar{g}] = S[\bar{g} + \hat{h}] + S_{\text{gf}}[\hat{h}; \bar{g}] + S_{\text{gh}}[\hat{h}, C, \bar{C}; \bar{g}]$ . In the path-integral we introduced the gauge-fixing term

$$S_{\text{gf}} = \frac{1}{2\alpha} \int d^d x \sqrt{\bar{g}} \bar{g}^{\mu\nu} F_\mu F_\nu, \quad (8)$$

which implements a suitable gauge-fixing condition  $F_\mu$ , and the corresponding ghost term

$$S_{\text{gh}}[\hat{h}, C, \bar{C}; \bar{g}] = -\kappa^{-1} \int d^d x \sqrt{\bar{g}} \bar{C}_\mu \bar{g}^{\mu\nu} \frac{\partial F_\nu}{\partial h_{\alpha\beta}} \mathcal{L}_C(\bar{g} + h), \quad (9)$$

which is obtained from the exponentiation of the Faddeev-Popov determinant. The path-integral has also been supplemented by source-terms for the fluctuation fields

$$S_{\text{source}} = - \int d^d x \sqrt{\bar{g}} \left[ t^{\mu\nu} \hat{h}_{\mu\nu} + \bar{\sigma}_\mu C^\mu + \sigma^\mu \bar{C}_\mu \right], \quad (10)$$

with which it is possible to construct general expectation values for the corresponding fields. The key ingredient for constructing the flow equation for the effective average action is the IR regulator  $\Delta_k S[\hat{h}, C, \bar{C}; \bar{g}]$  which suppresses fluctuations with momenta smaller than  $k^2$  by a  $k$ -dependent mass term. In order to explicitly maintain the background symmetry (6) at any stage, it is customary to implement the separation of high- and low-momentum modes in terms of the eigenvalues of a given covariant operator  $\square$ , which is constructed from the background metric and which encodes the propagation of the fluctuation fields. In the simplest case (known as Type I cutoff) one chooses the operator to be the background Laplacian  $\square = -\bar{D}^2$ , where the covariant derivative  $D_\mu$  is constructed using the Christoffel connection of the background, however, as we will show later on, other choices are admissible as well. Generically we choose the IR regulator to be quadratic

$$\Delta_k S = \frac{1}{2} \int d^d x \sqrt{\bar{g}} \hat{\phi} \mathcal{R}_k(\square) \hat{\phi}, \quad (11)$$

where  $\hat{\phi} = \{\hat{h}_{\mu\nu}, C^\mu, \bar{C}_\mu\}$  is the collection of fluctuation fields and  $\mathcal{R}_k$  is matrix valued in field space.

Introducing the  $k$ -dependent generating functional for the connected Green-functions,  $W_k = \ln Z_k$ , the vacuum expectation values of the fluctuation fields are given by the variations of  $W_k$  with respect to the corresponding source

$$h_{\mu\nu} = \frac{1}{\sqrt{\bar{g}}} \frac{\delta W_k}{\delta t^{\mu\nu}}, \quad \zeta^\mu = \frac{1}{\sqrt{\bar{g}}} \frac{\delta W_k}{\delta \bar{\sigma}_\mu}, \quad \bar{\zeta}_\mu = \frac{1}{\sqrt{\bar{g}}} \frac{\delta W_k}{\delta \sigma^\mu}, \quad (12)$$

and will collectively be denoted by  $\Phi^i \equiv \{\bar{h}_{\mu\nu}, \zeta^\mu, \bar{\zeta}_\mu\}$ . For completeness, we introduce  $g_{\mu\nu}$  as the classical analogue of (4)

$$g_{\mu\nu} = \bar{g}_{\mu\nu} + h_{\mu\nu}. \quad (13)$$

The effective average action  $\Gamma_k[\Phi^i, \bar{\Phi}^i]$  is then defined as the Legendre-transform of  $W_k$  up to the subtraction of the IR regulator evaluated on the

expectation values

$$\Gamma_k[\Phi^i, \bar{\Phi}^i] = \int d^d x \sqrt{\bar{g}} [t^{\mu\nu} h_{\mu\nu} + \bar{\sigma}_\mu \zeta^\mu + \sigma^\mu \bar{\zeta}_\mu] - W_k - \Delta_k S[\bar{h}_{\mu\nu}, \zeta^\mu, \bar{\zeta}_\mu; \bar{g}]. \quad (14)$$

Following the original derivation [8], one finds that the scale-dependence of the gravitational effective average action is encoded in the exact functional renormalization group equation (1). Inside (1),  $\Gamma_k^{(2)}$  denotes the second functional derivative of  $\Gamma_k$  with respect to the fluctuation fields

$$\Gamma_k^{(2)ij}(x, y) \equiv \frac{1}{\sqrt{\bar{g}(x)}} \frac{1}{\sqrt{\bar{g}(y)}} \frac{\delta^2 \Gamma_k}{\delta \Phi^i(x) \delta \Phi^j(y)}. \quad (15)$$

Eqs. (1) and (15) conclude our mini-review on the covariant flow equation for Quantum Einstein Gravity [8].

## 2.2. The geometrical flow equation

From a geometrical perspective the  $h_{\mu\nu}$  are coordinates on the configuration space of the system. For metric QEG this configuration space is given by the fiber bundle  $\text{Riem}(M)$  with the typical fiber being the diffeomorphism group  $\text{Diff}(M)$ . Physically inequivalent configurations span the base space  $\text{Riem}(M)/\text{Diff}(M)$  of the bundle.

In the previous subsection the sum over physically inequivalent configurations is constructed by performing the gauge-fixing (8) and adding the ghost action (9). In contrast to this gauge-fixing procedure, the geometric approach introduces coordinates on  $\text{Diff}(M)$  which are adjusted to the bundle structure: inequivalent physical configurations are described by their horizontal coordinates  $\hat{h}^A$  while gauge-equivalent configurations differ by their fiber coordinate  $\hat{\varphi}^\alpha$ . By construction the quantum gauge transformations (5) act along the fiber

$$\delta_Q \hat{h}^A = 0, \quad \delta_Q \hat{\varphi}^\alpha = \hat{\varphi}^{\alpha'}. \quad (16)$$

Since the action  $S[\gamma]$  is diffeomorphism invariant, the transformation entails that it must be independent of  $\hat{\varphi}^\alpha$ :  $S[\gamma] = S[\hat{h}^A; \bar{g}]$  [87]. As a consequence, the analogue of the partition sum (7) may be written as

$$\mathcal{Z}_k^{\text{geo}} \equiv \int \mathcal{D}\hat{\varphi}^\alpha \int \mathcal{D}\hat{h}^A \exp \left\{ -S[\hat{h}^A; \bar{g}] - \Delta_k S[\hat{h}^A; \bar{g}] - S_{\text{source}} \right\}. \quad (17)$$

In contrast to the metric construction  $\mathcal{Z}_k^{\text{geo}}$  does not include the gauge-fixing and ghost actions. Moreover, the IR-regulator is introduced for the gauge-invariant fields  $\hat{h}^A$  only. As a consequence the integration over the fibers becomes trivial and gives rise to an overall multiplicative factor. Using a suitable definition of  $\mathcal{D}\hat{\varphi}^\alpha$ , (17) is invariant with respect to *both* background and quantum gauge transformations.

Introducing the expectation values  $h^A \equiv \langle \hat{h}^A \rangle$  and following the derivation of the previous subsection step by step one obtains the geometric version of the FRGE for Quantum Einstein Gravity

$$\partial_t \Gamma_k[h^A; \bar{g}] = \frac{1}{2} \text{Tr} \left[ \left( \Gamma_k^{(2)} + \mathcal{R}_k \right)^{-1} \partial_t \mathcal{R}_k \right]. \quad (18)$$

While this equation has the same structural form as (1) the crucial difference is the form of the Hessian  $\Gamma_k^{(2)}$ . While the Hessian of the previous construction is with respect to  $\Phi^i = \{h_{\mu\nu}, \zeta^\mu, \bar{\zeta}_\mu\}$  the  $\Gamma_k^{(2)}$  appearing in the geometric flow equation contains the gauge-invariant fields  $h^A$  only

$$\Gamma_k^{(2)AB}(x, y) \equiv \frac{1}{\sqrt{\bar{g}(x)}} \frac{1}{\sqrt{\bar{g}(y)}} \frac{\delta^2 \Gamma_k}{\delta h^A(x) \delta h^B(y)}. \quad (19)$$

The flow equation (18) is the central result of this subsection. Just like its metric twin, it is an exact equation in the sense that it contains the same information as the path integral (17). No approximation has been made in its derivation. Obviously, eq. (18) is independent of the choice of gauge-fixing and does not depend on ghost-fields. As its major advantage it is *invariant under both background and quantum gauge transformations*.

Analogously to the metric flow equation, the solutions of (17) interpolate between the bare action  $S[g]$  for  $k \rightarrow \infty$  and the standard (off-shell) effective action  $\Gamma = \Gamma_{k=0}$  in the IR. Naturally, all approximation schemes, as, e.g., the derivative expansion or the vertex expansion, which have been used to construct approximate solutions of (1) can also be applied to (17). In Sects. 3 and 5 we will carry out a first set of checks, verifying that the geometric flow equation and the metric FRGE leads to similar results.

### 2.3. Coordinates on the configuration space

While the geometrical flow equation (18) is conceptually nice, its practical usefulness hinges on being able to construct the map

$$h_{\mu\nu} \mapsto \{ h^A, \varphi^\alpha \} \quad (20)$$

relating the fluctuation field to the coordinates  $h^A$  and  $\varphi^\alpha$  on the base space and fiber of the gauge-bundle. In principle, this map can be constructed by introducing Vilkovisky's connection [88, 87] and following the construction [89], also see [90] for a more pedagogical exposition and [73] for a related discussion in the context of the FRGE.

Here we will follow a different path and advocate to construct “approximately gauge-invariant fields” via a specific coordinate transformation on the configuration space. Our starting point is the observation that the quantum gauge transformations (5) acting on  $h_{\mu\nu}$  is given by

$$\begin{aligned} \delta_Q h_{\mu\nu} &= D_\mu v_\nu + D_\nu v_\mu \\ &= D_\mu v_\nu^T + D_\nu v_\mu^T + 2D_\mu D_\nu v. \end{aligned} \quad (21)$$

Here we have performed the decomposition of the coordinate transformation  $v_\mu = v_\mu^T + D_\mu v$  into its transverse and longitudinal components *with respect to*  $g_{\mu\nu}$  in the second line. In order to obtain the relation between  $h_{\mu\nu}$  and the adapted coordinate system on the gauge bundle  $\{h^A, \varphi^\alpha\}$  we consider the implicit change of coordinates

$$h_{\mu\nu} = \tilde{h}_{\mu\nu}^T + D_\mu \tilde{\xi}_\nu + D_\nu \tilde{\xi}_\mu + 2D_\mu D_\nu \tilde{\sigma} - \frac{1}{d} g_{\mu\nu} \tilde{\chi}, \quad (22)$$

where  $h_{\mu\nu}[\tilde{h}_{\mu\nu}^T, \tilde{\xi}_\nu, \tilde{\sigma}, \tilde{\chi}; \bar{g}]$  is understood as a functional of the component fields  $\{\tilde{h}_{\mu\nu}^T, \tilde{\xi}_\nu, \tilde{\sigma}, \tilde{\chi}\}$  and the background metric  $\bar{g}$ . Here  $\tilde{\chi} = \tilde{h} - 2D^2 \tilde{\sigma}$  and the component fields satisfy the constraints

$$D^\mu \tilde{h}_{\mu\nu}^T = 0, \quad g^{\mu\nu} \tilde{h}_{\mu\nu}^T = 0, \quad D_\mu \tilde{\xi}^\mu = 0, \quad g^{\mu\nu} h_{\mu\nu} = \tilde{h}. \quad (23)$$

Comparing (21) with (22) one establishes that the component fields inherit the transformation law

$$\tilde{h}_{\mu\nu}^T \mapsto \tilde{h}_{\mu\nu}^T, \quad \tilde{\xi}_\mu \mapsto \tilde{\xi}_\mu + v_\mu^T, \quad \tilde{\sigma} \mapsto \tilde{\sigma} + v, \quad \tilde{\chi} \mapsto \tilde{\chi}. \quad (24)$$

Thus

$$h^A = \left\{ \tilde{h}_{\mu\nu}^T, \tilde{\chi} \right\}, \quad \varphi^\alpha = \left\{ \tilde{\xi}_\mu, \tilde{\sigma} \right\}, \quad (25)$$

is the desired trivialization of the configuration space.

Notably the relation (22) is exact and, so far, no approximation has been made: the relation gives an *implicit equation* between the metric fluctuations  $h_{\mu\nu}$  and the coordinates  $\{h^A, \varphi^\alpha\}$  trivializing the configuration space. Since the r.h.s. contains the inverse metric  $g^{\mu\nu}$  this relation is highly non-linear and non-local in the sense that the relation involves terms containing an infinite number of derivatives. This reflects the common folklore that there are no local, gauge-invariant observables in quantum gravity [91]. Formally, the relation may be solved for the component fields by applying the projection operators of the transverse-traceless (TT) decomposition [72], replacing  $\bar{g}_{\mu\nu}$  with  $g_{\mu\nu}$ .<sup>2</sup> These operators involve the inverse of local differential operators, making the non-local nature of the decomposition manifest.

Instead of working with the exact relation (22), we follow the suggestion [91] and use the implicit relation to construct “approximately gauge-invariant fluctuation fields”. This strategy actually fits well into the typical approximations used to evaluate RG flows with the FRGE by performing a derivative expansion and limiting the power of the fluctuation fields kept

---

<sup>2</sup>In the case where the TT decomposition is with respect to a fixed background  $\bar{g}_{\mu\nu}$  the uniqueness of the decomposition (up to possible Killing- and conformal Killing vectors of the background) has been established in [72]. We are not aware of similarly stringent mathematical results for the decomposition (22). The fact that (22) can be solved by a bootstrap procedure order by order in the fluctuation fields, hints at the possibility that the decomposition is indeed unique.

track in the flow (“single-metric vs. “bi-metric” expansions). Concretely, we will limit ourselves to construct the relation between  $h_{\mu\nu}$  and the coordinates (25) to linear order. For this purpose, it is useful to perform the standard TT or York-decomposition of the fluctuation fields with respect to the background metric  $\bar{g}_{\mu\nu}$ :

$$h_{\mu\nu} = h_{\mu\nu}^{\text{T}} + \bar{D}_\mu \xi_\nu + \bar{D}_\nu \xi_\mu + 2\bar{D}_\mu \bar{D}_\nu \sigma - \frac{2}{d} \bar{g}_{\mu\nu} \bar{D}^2 \sigma + \frac{1}{d} \bar{g}_{\mu\nu} h, \quad (26)$$

where the component fields are subject to the constraints

$$\bar{D}^\mu h_{\mu\nu}^{\text{T}} = 0, \quad \bar{g}^{\mu\nu} h_{\mu\nu}^{\text{T}} = 0, \quad \bar{D}_\mu \xi^\mu = 0, \quad \bar{g}^{\mu\nu} h_{\mu\nu} = h. \quad (27)$$

Again the terms proportional to  $\bar{g}_{\mu\nu}$  can conveniently be combined by introducing the new field

$$\chi = h - 2\bar{D}^2 \sigma. \quad (28)$$

Notably, the r.h.s. of (22) and (26) coincide at linear order in the fluctuation fields. Thus, at linear order, the coordinates trivializing the configuration space are given by the component fields of the TT-decomposition:

$$h^1 = h_{\mu\nu}^{\text{T}} + \mathcal{O}(h^2), \quad h^2 = \chi + \mathcal{O}(h^2), \quad \varphi^1 = \xi_\mu + \mathcal{O}(h^2), \quad \varphi^2 = \sigma + \mathcal{O}(h^2). \quad (29)$$

Thus, at this level of approximation the gauge-invariant fields  $h^A = \{h_{\mu\nu}^{\text{T}}, \chi\}$  are given by the component fields of the TT-decomposition and the variations in (18) are with respect to the transverse-traceless field and scalar  $\chi$  only.

At this stage, the following remark is in order. In order to correctly make the transition from the gauge-dependent to the gauge-independent coordinates the knowledge of higher-order terms in the map (29) is required. A correct single-metric computation (which, by definition, evaluates (1) at  $h_{\mu\nu} = 0$ ) requires knowing the quadratic corrections to (29). Consequently, the study of vertex functions including  $N$  fluctuation fields (baptized bi-metric computations in [43, 44, 45]) needs the map up to order  $N + 2$ . The  $N$ th variation of  $h_{\mu\nu}$  with respect to the fields  $\{\tilde{h}_{\mu\nu}^{\text{T}}, \tilde{\chi}, \tilde{\xi}_\mu, \tilde{\sigma}\}$  can be constructed systematically from (22) by constructing the variations recursively through a bootstrap procedure. The construction of these terms is beyond the scope of the present paper and we will limit our computations to the linear approximation (29).

#### 2.4. The flow equation in Landau-De Witt gauge

The flow equation (18) in combination with the linearized geometric approximation (29) can also be obtained from the standard gauge-fixed covariant flow equation for QEG (1), provided that the integration variables in the path integral are given by the component fields of the TT-decomposition and that one evaluates (1) at zero-order in the fluctuation field [92]. The

first requirements avoids introducing Jacobi-determinants from the field re-definition while the second approximation allows the explicit cancellation between the traces containing the gauge- and ghost degrees of freedom.

In order to arrive at (18) one starts from an ansatz for the effective average action where the gauge-fixing and ghost terms retain their classical form

$$\Gamma_k[\bar{h}, \bar{\zeta}, \zeta; \bar{g}] = \Gamma_k^{\text{grav}}[\bar{h}; \bar{g}] + S_{\text{gf}}[\bar{h}; \bar{g}] + S_{\text{gh}}[\bar{h}, \bar{\zeta}, \zeta; \bar{g}]. \quad (30)$$

For the disentanglement of the physical and gauge degrees of freedom we resort to the so-called minimal TT-decomposition [55], which refrains from splitting the vector field into its transverse and longitudinal parts

$$h_{\mu\nu} = h_{\mu\nu}^{\text{T}} + \bar{D}_\mu \rho_\nu + \bar{D}_\nu \rho_\mu - \frac{2}{d} \bar{g}_{\mu\nu} \bar{D}^\alpha \rho_\alpha + \frac{1}{d} \bar{g}_{\mu\nu} h. \quad (31)$$

The vector field  $\rho_\nu$  is related to the component fields appearing in (26) by

$$\rho_\mu = \xi_\mu + \bar{D}_\mu \sigma. \quad (32)$$

and thus captures the gauge degrees of freedom at the linear level. The gauge fixing condition is then chosen to be geometrical Landau-De Witt gauge [93, 22, 23]

$$F_\mu = \bar{D}^\nu \bar{h}_{\mu\nu} - \frac{1}{d} \bar{D}_\mu h = \mathcal{F}[\bar{g}]_\mu{}^\nu \rho_\nu, \quad (33)$$

with

$$\mathcal{F}[\bar{g}]_\mu{}^\nu = \delta_\mu^\nu \bar{D}^2 + \frac{d-2}{2d} (\bar{D}^\nu \bar{D}_\mu + \bar{D}_\mu \bar{D}^\nu) + \frac{d+2}{2d} \bar{R}_\mu^\nu. \quad (34)$$

Thus, for this particular gauge choice  $F_\mu$  is independent of  $h_{\mu\nu}^{\text{T}}$  and  $h$  and contains  $\rho_\nu$  only. Moreover,  $\mathcal{F}$  is hermitian with respect to the “scalar product”  $\int d^d x \sqrt{\bar{g}}$ , so that

$$S_{\text{gf}} = \frac{1}{2\alpha} \int d^d x \sqrt{\bar{g}} \rho_\mu \mathcal{G}^\mu{}_\nu \rho^\nu. \quad (35)$$

with  $\mathcal{G} = \mathcal{F}^2$ . Setting the background ghosts to zero, the part of the ghost action quadratic in the fluctuation fields becomes

$$S_{\text{gh}} = - \int d^d x \sqrt{\bar{g}} \bar{\zeta}_\mu \mathcal{M}^\mu{}_\nu \zeta^\nu. \quad (36)$$

with

$$\mathcal{M}^\mu{}_\nu = \delta_\mu^\nu \bar{D}^2 + \frac{d-2}{2d} (\bar{D}^\nu \bar{D}_\mu + \bar{D}_\mu \bar{D}^\nu) + \frac{d+2}{2d} \bar{R}_\mu^\nu. \quad (37)$$

Thus, for this particular gauge-fixing the ghost operator (at zeroth order in the fluctuation field) agrees with the gauge fixing operator,  $\mathcal{F} = \mathcal{M}$ .

In the next step, we impose the Landau-De Witt gauge, taking the gauge parameter  $\alpha \rightarrow 0$ . In this limit the Hessian  $\Gamma_k^{(2)ij}$ , given in (15), becomes block-diagonal. The dynamics of the gravitational sector is governed by the Hessian  $\Gamma_k^{(2)AB}$ , evaluated in the linear geometric approximation, while the contributions of the gauge-degrees of freedom is determined by the kernel  $\mathcal{G}$  of  $S_{\text{gf}}$

$$\begin{aligned} \partial_t \Gamma_k[h^A, \rho, \bar{\zeta}, \zeta; \bar{g}] &= \frac{1}{2} \text{Tr} \left( \Gamma_k^{(2)AB} + \mathcal{R}_k^{AB} \right)^{-1} \partial_t \mathcal{R}_k^{AB} \\ &+ \frac{1}{2} \text{Tr} \left( \mathcal{G} + \mathcal{R}_k^{\mathcal{G}} \right)^{-1} \partial_t \mathcal{R}_k^{\mathcal{G}} - \text{Tr} \left( \mathcal{M} + \mathcal{R}_k^{\text{gh}} \right)^{-1} \partial_t \mathcal{R}_k^{\text{gh}}. \end{aligned} \quad (38)$$

The first line is the r.h.s. of the geometric flow equation in the linear geometric approximation. The special gauge choice  $\mathcal{G} = \mathcal{F}^2$  with  $\mathcal{F} = \mathcal{M}$  implies moreover, that the traces in the second line may cancel for a specific choice of regulator. Indeed setting

$$\mathcal{R}_k^{\mathcal{G}} = \left( \mathcal{R}_k^{\text{gh}} \right)^2 + \mathcal{M} \mathcal{R}_k^{\text{gh}} + \mathcal{R}_k^{\text{gh}} \mathcal{M}, \quad (39)$$

and taking into account that  $\mathcal{M}$  is independent of the RG-scale  $k$  one has

$$\frac{1}{2} \text{Tr} \left( \mathcal{G} + \mathcal{R}_k^{\mathcal{G}} \right)^{-1} \partial_t \mathcal{R}_k^{\mathcal{G}} - \text{Tr} \left( \mathcal{M} + \mathcal{R}_k^{\text{gh}} \right)^{-1} \partial_t \mathcal{R}_k^{\text{gh}} = 0. \quad (40)$$

It can easily be checked that if  $\mathcal{R}_k^{\text{gh}}$  is a regulator then also  $\mathcal{R}_k^{\mathcal{G}}$  fulfills all properties required of an admissible regulator function. This is the “mode-by-mode” cancellation between gauge-degrees of freedom and ghost modes used in [22].

For the particular choice of regulator (38) reduces to (18) subject to the approximation (29). Thus the geometric flow equation evaluated in the linear geometric approximation may also be obtained as a particular truncation of the gauge-fixed FRGE (1) with very specific choices for the gauge-fixing function and regulators. At this stage we stress that the geometric flow equation (18) is, in principle, an exact flow equation for Quantum Einstein Gravity having the same information content as the standard FRGE but at the same time being manifestly invariant under background and quantum gauge-transformations. The RG flows obtained from this flow equation, subject to the linear geometric approximation, will be analyzed in the remaining sections.

### 3. The Einstein-Hilbert truncation

As a first illustration of the RG flows implied by (18), we work out the single-metric Einstein-Hilbert truncation [8, 15, 16] in the linear-geometric

approximation. The corresponding ansatz for the effective average action,

$$\Gamma_k[h^A; \bar{g}] = \frac{1}{16\pi G_k} \int d^d x \sqrt{\bar{g}} \{2\Lambda_k - R\}, \quad (41)$$

contains the scale-dependent Newton's constant  $G_k$  and cosmological constant  $\Lambda_k$ . Note that in the geometrical formalism  $\Gamma_k$  is *not* supplemented by a gauge-fixing and ghost action and contains  $\Gamma_k^{\text{grav}}[g]$  only.

Substituting the ansatz (41) into (18) and setting the fluctuation field to zero afterwards, the l.h.s. of the equation becomes

$$\partial_t \Gamma_k[\bar{g}] = \int d^d x \sqrt{\bar{g}} \left\{ 2 \partial_t \left( \frac{\Lambda_k}{16\pi G_k} \right) - \bar{R} \partial_t (16\pi G_k)^{-1} \right\}. \quad (42)$$

Thus the scale-dependence of Newton's constant and the cosmological constant is encoded in the coefficients multiplying the volume term and the interaction term linear in the background Ricci scalar  $\bar{R}$ . In order to distinguish between these terms, it suffices to carry out the computation for the background metric being the one of the  $d$ -dimensional sphere, so that the background curvature tensors satisfy (A.1). While the same result can also be obtained without making a specific choice for  $\bar{g}_{\mu\nu}$  [55], this choice tremendously simplifies the computation and will be adopted throughout the rest of the paper.

The beta functions for  $G_k$  and  $\Lambda_k$  are obtained by evaluating the r.h.s. of the flow equation up to linear order in the background curvature. The first step expands the ansatz (41) to second order in the fluctuation fields. In the linear-geometric approximation where  $h^A = \{h_{\mu\nu}^T, \chi\}$ ,  $h^\alpha = \{\xi_\mu, \sigma\}$  the quadratic term in this expansion is

$$\begin{aligned} \Gamma_k^{\text{quad}}[h^A; \bar{g}] = \frac{1}{64\pi G_k} \int d^d x \sqrt{\bar{g}} \left\{ h_{\mu\nu}^T [\Delta - 2\Lambda_k + c_T \bar{R}] h^{\text{T}\mu\nu} \right. \\ \left. - \frac{(d-2)(d-1)}{2} \chi \left[ \Delta - \frac{d}{d-1} \Lambda_k + c_S \bar{R} \right] \chi \right\} \end{aligned} \quad (43)$$

with

$$c_T \equiv \frac{d^2 - 3d + 4}{d(d-1)}, \quad c_S \equiv \frac{d-4}{2(d-1)}. \quad (44)$$

Thus the Hessian (19) obtained from (43) is diagonal in field space.

The next step is the construction of the regulator  $\mathcal{R}_k$ . For definiteness, we choose the coarse-graining operator  $\square = \Delta$  and implement a Type I regulator scheme [24]. In this case  $\mathcal{R}_k$  is determined by the replacement rule  $\Delta \mapsto P_k \equiv \Delta + R_k$  with  $R_k$  a scalar cutoff function suppressing low-energy fluctuations by a mass-term. This implicit definition fixes

$$\mathcal{R}_k = \frac{1}{32\pi G_k} \text{diag} \left[ R_k \mathbf{1}, -\frac{(d-2)(d-1)}{2} R_k \right]. \quad (45)$$

The truncated flow equation resulting from the ansatz (41) then reads

$$\partial_t \Gamma_k[\bar{g}] = \frac{1}{2} T_{(2)} + \frac{1}{2} T_{(0)} \quad (46)$$

with the traces  $T_{(s)}$  in the transverse-traceless ( $s = 2$ ) and scalar ( $s = 0$ ) sector given by

$$\begin{aligned} T_{(2)} &= \text{Tr}_{(2)} \left[ \left( P_k - 2\Lambda_k + c_T \bar{R} \right)^{-1} \left( \partial_t R_k - \eta R_k \right) \right], \\ T_{(0)} &= \text{Tr}_{(0)} \left[ \left( P_k - \frac{d}{d-1} \Lambda_k + c_S \bar{R} \right)^{-1} \left( \partial_t R_k - \eta R_k \right) \right]. \end{aligned} \quad (47)$$

Here  $\eta \equiv \partial_t \ln G_k$  denotes the anomalous dimension of Newtons constant.

The evaluation of the traces up to linear order in the background curvature is readily done by applying the trace technology of Appendix A.1. Expanding the trace arguments in  $\bar{R}$ , the functions  $W(\Delta)$  entering into eq. (A.6) are of the form

$$W_m(z; w) \equiv (P_k + w)^{-m} (\partial_t R_k - \eta R_k). \quad (48)$$

This motivates defining

$$Q_n^m(w) \equiv Q_n [W_m(z; w)]. \quad (49)$$

Applying the expansion (A.6) and retaining the terms contained in the ansatz (41) only, the traces (47) give

$$\begin{aligned} T_{(2)} &= \frac{1}{(4\pi)^{d/2}} \int d^d x \sqrt{\bar{g}} \left[ Q_{d/2}^1(-2\Lambda_k) b_0^{(2)} \right. \\ &\quad \left. + \left( Q_{d/2-1}^1(-2\Lambda_k) b_1^{(2)} - c_T Q_{d/2}^2(-2\Lambda_k) b_0^{(2)} \right) \bar{R} \right], \\ T_{(0)} &= \frac{1}{(4\pi)^{d/2}} \int d^d x \sqrt{\bar{g}} \left[ Q_{d/2}^1 \left( -\frac{d\Lambda_k}{d-1} \right) b_0^{(0)} \right. \\ &\quad \left. + \left( Q_{d/2-1}^1 \left( -\frac{d\Lambda_k}{d-1} \right) b_1^{(0)} - c_S Q_{d/2}^2 \left( -\frac{d\Lambda_k}{d-1} \right) b_0^{(0)} \right) \bar{R} \right], \end{aligned} \quad (50)$$

with the coefficients  $b_n^{(s)}$  given in (A.5).

The beta functions capturing the scale-dependence of  $G_k$  and  $\Lambda_k$  are then obtained by substituting (42) and (50) into (46) and equating the coefficients multiplying different powers of the scalar curvature. The result is most conveniently expressed in terms of the dimensionless coupling constants

$$\lambda_k \equiv \Lambda_k k^{-2}, \quad g_k \equiv G_k k^{d-2}, \quad (51)$$

and reads

$$\partial_t g_k = \beta_g(g, \lambda), \quad \partial_t \lambda_k = \beta_\lambda(g, \lambda), \quad (52)$$

with

$$\begin{aligned}\beta_g &= (d-2+\eta)g \\ \beta_\lambda &= (\eta-2)\lambda + \frac{g}{(4\pi)^{d/2-1}} \left[ (d-2)(d+1)\Phi_{d/2}^1(-2\lambda) + 2\Phi_{d/2}^1\left(-\frac{d\lambda}{d-1}\right) \right. \\ &\quad \left. - \eta \left( \frac{(d-2)(d+1)}{2} \tilde{\Phi}_{d/2}^1(-2\lambda) + \tilde{\Phi}_{d/2}^1\left(-\frac{d\lambda}{d-1}\right) \right) \right].\end{aligned}\tag{53}$$

The explicit expression for the anomalous dimension of Newton's constant is given by

$$\eta = \frac{gB_1(\lambda)}{1-gB_2(\lambda)},\tag{54}$$

with

$$\begin{aligned}B_1(\lambda) &= \frac{1}{(4\pi)^{d/2-1}} \left[ \frac{(d^2+3d+2)(3\delta_{d,2}+d-5)}{3(d-1)} \Phi_{d/2-1}^1(-2\lambda) + \frac{2}{3} \Phi_{d/2-1}^1\left(-\frac{d\lambda}{d-1}\right) \right. \\ &\quad \left. - \frac{2(d^4-4d^3+5d^2+2d-8)}{d(d-1)} \Phi_{d/2}^2(-2\lambda) - \frac{2(d-4)}{d-1} \Phi_{d/2}^2\left(-\frac{d\lambda}{d-1}\right) \right] \\ B_2(\lambda) &= \frac{1}{(4\pi)^{d/2-1}} \left[ -\frac{(d^2+3d+2)(3\delta_{d,2}+d-5)}{6(d-1)} \tilde{\Phi}_{d/2-1}^1(-2\lambda) - \frac{1}{3} \tilde{\Phi}_{d/2-1}^1\left(-\frac{d\lambda}{d-1}\right) \right. \\ &\quad \left. + \frac{(d^4-4d^3+5d^2+2d-8)}{d(d-1)} \tilde{\Phi}_{d/2}^2(-2\lambda) + \frac{d-4}{d-1} \tilde{\Phi}_{d/2}^2\left(-\frac{d\lambda}{d-1}\right) \right]\end{aligned}\tag{55}$$

In these expressions, the dependence of the beta functions on the regulator is captured by the dimensionless threshold functions

$$\begin{aligned}\Phi_n^m(w) &\equiv \frac{1}{\Gamma(n)} \int_0^\infty dy y^{n-1} \frac{\varrho(y) - y\varrho'(y)}{(y + \varrho(y) + w)^m}, \\ \tilde{\Phi}_n^m(w) &\equiv \frac{1}{\Gamma(n)} \int_0^\infty dy y^{n-1} \frac{\varrho(y)}{(y + \varrho(y) + w)^m},\end{aligned}\tag{56}$$

where  $\varrho(y)$  denotes the dimensionless profile function of the cutoff,  $R_k = k^2\varrho(zk^{-2})$ . These threshold functions are related to the  $Q$ -functionals (49) by

$$Q_n^m(w) = k^{2(n-m)+2} \left[ 2\Phi_n^m(w/k^2) - \eta \tilde{\Phi}_n^m(w/k^2) \right].\tag{57}$$

The beta functions (53) together with the expression for the anomalous dimension of Newton's constant (54) constitute the main result of this section.

For the remainder of this section we then study the properties of the flow implied by (52). For this purpose we set  $d=4$  and chose the optimized regulator [94]

$$\varrho(z) = (1-z)\theta(1-z).\tag{58}$$

For this choice of regulator, the integrals appearing in the threshold functions can be performed analytically, yielding

$$\Phi_n^m(w) = \frac{1}{\Gamma(n+1)} \frac{1}{(1+w)^m}, \quad \tilde{\Phi}_n^m(w) = \frac{1}{\Gamma(n+2)} \frac{1}{(1+w)^m}. \quad (59)$$

The most important feature of an RG flow are its fixed points (FPs)  $g_*$  where, by definition, all beta functions vanish simultaneously  $\beta_{g_i}|_{g=g_*} = 0$ . Given a FP, the dynamics of the RG flow in its vicinity is captured by the linearized system

$$\partial_t g_i = \mathbf{M}_{ij} (g_j - g_{j*}), \quad (60)$$

governed with the stability matrix

$$\mathbf{M}_{ij} = \left. \frac{\partial \beta_{g_i}}{\partial g_j} \right|_{g=g_*}. \quad (61)$$

The critical exponents  $\theta_i$ , defined as minus the eigenvalues of  $\mathbf{M}$ , are a characteristic feature of the FP, identifying its universality class. In particular they encode whether a perturbation of the FP theory is UV relevant ( $\text{Re}(\theta) > 0$ ), irrelevant ( $\text{Re}(\theta) < 0$ ), or marginal ( $\text{Re}(\theta) = 0$ ).

Inspecting the beta functions (53), one finds that the system possesses a so-called Gaussian Fixed Point (GFP)

$$\text{GFP} : \quad g_* = 0, \quad \lambda_* = 0. \quad (62)$$

This point corresponds to a non-interacting theory and the critical exponents of the fixed point match the mass dimension of the coupling constants. In addition, the beta functions possess a non-Gaussian Fixed Point (NGFP) with  $g_* > 0, \lambda_* > 0$ . The position and characteristic properties of this fixed point obtained from applying the linear-geometric approximation to the Einstein-Hilbert truncation are summarized in the first line of Table 1. For comparison we also include the characteristic properties of the NGFP found in previous literature studies supplementing the Einstein-Hilbert action by gauge-fixing and ghost terms. Notably, the geometric flow recovers all the characteristic properties found previously, including the complex pair of critical exponents  $\theta_{1,2} = \theta' \pm i\theta''$ . Moreover, the universal combination  $g_*\lambda_*$  essentially agrees with the value found in the full, gauge-fixed case. We take these findings as a strong indication that the properties of the NGFP are largely governed by the transverse-traceless and trace-sectors of the flow equation while the gauge-fixing and ghost contributions play a minor role only.

In addition to studying the characteristic features of the NGFP appearing in the linearized geometric approximation, we also construct the phase diagram obtained from integrating the flow (52). The flow is shown in Fig. 1. For  $g_k > 0$  it is governed by the interplay between the NGFP, governing the

| $g_*$ | $\lambda_*$ | $g_*\lambda_*$ | $\theta'$ | $\theta''$ |                             |
|-------|-------------|----------------|-----------|------------|-----------------------------|
| 0.781 | 0.203       | 0.16           | 2.929     | 2.965      | linear geometric flow       |
| 0.272 | 0.348       | 0.12           | 1.547     | 3.835      | TT-decomposition            |
| 0.403 | 0.330       | 0.13           | 1.941     | 3.147      | harmonic gauge              |
| 1.178 | 0.25        | 0.29           | 1.667     | 4.308      | optimized flow              |
| 0.893 | 0.164       | 0.146          | 2.03      | 2.69       | geometrical background flow |
| 1.692 | 0.144       | 0.244          | 1.34      | 2.61       | geometrical dynamical flow  |
| 2.665 | 0.415       | 1.11           | 1.471     | 9.304      | CREH (pot)                  |
| 4.650 | 0.279       | 1.30           | 4.0       | 6.184      | CREH (kin)                  |

Table 1: Characteristic features of the NGFP appearing in Einstein-Hilbert truncation. The results based on the linear geometric approximation introduced in this work are given in the first line. The lower lines show characteristics of the NGFP obtained from the gauge-fixed Einstein-Hilbert truncation [8, 15, 16, 95, 18] and the conformally reduced Einstein-Hilbert (CREH) truncation [37] for comparison.

UV-behavior of the theory, and GFP controlling its IR-regime. The phase diagram qualitatively displays all the features encountered in previous RG studies based on the Einstein-Hilbert truncation [16]. The qualitative match of the fixed point characteristics and phase diagrams provides a strong indication that our new flow equation based on gauge-invariant fields (18) indeed captures all essential features of the gravitational RG flow even in the case where the linear geometric approximation (29) is invoked. In particular, the results are significantly closer to the gauge-fixed computations than the one taking into account the contribution of the conformal factor only (CREH).

#### 4. The $f(R)$ -truncation: flow equation

Upon completing our analysis of the RG flows obtained from the Einstein-Hilbert truncation in the linear-geometric approximation, we shall now derive the partial differential equation (PDE) governing the RG flow of  $f(R)$ -gravity. The essentially new ingredient in the derivation is the inclusion of non-trivial endomorphisms in the regulator. We will find that the choice of endomorphism may alter the singularity structure of the flow equation, so that the existence of isolated fixed functionals becomes admissible.

The  $f(R)$ -truncation approximates the effective average action by

$$\Gamma_k[h^A; \bar{g}] = \int d^d x \sqrt{\bar{g}} f_k(R). \quad (63)$$

Again the ansatz for  $\Gamma_k$  depends on the gauge-invariant fluctuation fields  $h^A = \{h_{\mu\nu}^T, \chi\}$  only and does not include gauge-fixing and ghost-terms. The ansatz generalizes (41) by including infinitely many scale-dependent couplings and thus captures significantly more information about Asymptotic Safety, for instance concerning the predictive power of the construction.

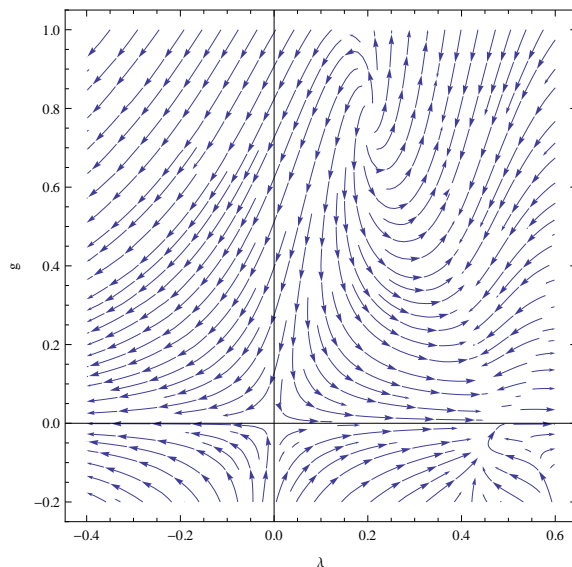


Figure 1: The flow of the dimensionless cosmological constant  $\lambda_k$  and Newton's coupling  $g_k$ . The arrows point towards the IR, i.e. decreasing values of  $k$ .

The construction of the PDE governing the scale-dependence of  $f_k(R)$  essentially parallels the computation of the beta functions for the Einstein-Hilbert truncation. Substituting the ansatz (63) into the geometric flow equation (18) and subsequently setting the fluctuation fields to zero the l.h.s. becomes

$$\partial_t \Gamma_k = \int d^d x \sqrt{\bar{g}} \partial_t f_k(\bar{R}). \quad (64)$$

This implies in particular that we can again choose the background metric to be the one of the  $d$ -sphere  $S^d$ , which suffices to project the exact RG flow on subspace spanned by the ansatz (63). In this background the part of  $\Gamma_k$  quartic in gauge invariant quantities  $h^A = \{h_{\mu\nu}^T, \chi\}$  is given by

$$\begin{aligned} \Gamma_k^{\text{quad}}[h^A; \bar{g}] = \frac{1}{2} \int d^d x \sqrt{\bar{g}} \left\{ -\frac{1}{2} h_{\mu\nu}^T \left[ \left( \Delta - \frac{2(d-2)}{d(d-1)} \bar{R} \right) f' + f \right] h^{\text{T}\mu\nu} \right. \\ \left. + \frac{d-2}{4d} \chi \left[ \frac{4(d-1)^2}{d(d-2)} \Delta_1^2 f'' + \frac{2(d-1)}{d} \Delta_2 f' + f \right] \chi \right\}, \end{aligned} \quad (65)$$

Here the prime denotes a derivative with respect to  $\bar{R}$  and we omitted the  $k$ - and  $\bar{R}$ -dependences of  $f_k(\bar{R})$  for notational clarity. In the second line we introduced the abbreviation  $\Delta_n \equiv \Delta - \frac{n\bar{R}}{d-1}$ .

The next step consists in constructing the regulator  $\mathcal{R}_k$ . Here we generalize the computation of the last section by allowing for a non-trivial spin-

dependent endomorphism  $E_{(s)}$  in the coarse-graining operator:

$$\square \equiv -\bar{D}^2 + E_{(s)}. \quad (66)$$

For practical reasons, we assume that  $E_{(s)}$  is covariantly constant with respect to  $\bar{D}_\mu$ . Including  $E_{(s)}$  brings the advantage that one can shift the value  $k_0$  where all fluctuation fields are integrated out. In particular the choice

$$E_{(0)} = E_{(2)} + \frac{2}{d-1} \bar{R} \quad (67)$$

entails that the fluctuations in the scalar ( $s = 0$ ) and transverse-traceless ( $s = 2$ ) coming with the lowest eigenvalues are integrated out at the same value  $k_0$ . Regulators that obey the relation (67) thus satisfy the condition of equal lowest eigenvalues (ELE). Subsequently, we define the regulator  $\mathcal{R}_k$  by the replacement rule  $\square \mapsto P_k(\square) \equiv \square + R_k(\square)$ . This implicit definition entails

$$\mathcal{R}_k = \text{diag} \left[ R_k^{(2)} \mathbf{1}, R_k^{(0)} \right], \quad (68)$$

with

$$\begin{aligned} R_k^{(2)} &= -\frac{1}{2} (P_k - \square) f', \\ R_k^{(0)} &= \frac{(d-1)^2}{d^2} \left( f'' (P_k^2 - \square^2) + \left( \frac{d-2}{2(d-1)} f' - 2 \left( E_{(0)} + \frac{\bar{R}}{d-1} \right) f'' \right) (P_k - \square) \right). \end{aligned} \quad (69)$$

We will now specialize to the case  $d = 4$ . The projected flow equation is then again of the form (46) with the transverse-traceless and scalar trace given by

$$\begin{aligned} T_{(2)} &= 6 \text{Tr} \left[ \frac{\partial_t R_k^{(2)}}{(3E_{(2)} + \bar{R} - 3P_k) f' - f} \right], \\ T_{(0)} &= 16 \text{Tr} \left[ \frac{\partial_t R_k^{(0)}}{(3E_{(0)} + \bar{R} - 3P_k)^2 f'' - (3E_{(0)} + 2\bar{R} - 3P_k) f' + 2f} \right]. \end{aligned} \quad (70)$$

For vanishing endomorphisms these traces coincide with the transverse-traceless and scalar sectors of the flow equations in the  $f(R)$ -truncation derived in [23, 24]. The crucial difference to these works is the inclusion of an arbitrary endomorphism in the regulator (Type II cutoff) and the absence of the auxiliary sector, capturing the Jacobians from the transverse-traceless decomposition of the metric fields.

The operator traces (70) depend on the coarse-graining operator  $\square$  and can be evaluated by slightly modifying eq. (A.3)

$$\text{Tr} [W(\square)] = \int_0^\infty d\sigma \widetilde{W}(\sigma) e^{-\sigma E_{(s)}} \text{Tr} [e^{-\sigma \Delta}]. \quad (71)$$

Here  $\widetilde{W}$  denotes the inverse Laplace transform of  $W$  and we have used that the endomorphism  $E_{(s)}$  is covariantly constant in order to extract it from the operator trace. The factor  $\mathbb{T}_{E_{(s)}} \equiv e^{-\sigma E_{(s)}}$  represents the translation operator on Laplace space. It acts on functions by a shift of their argument  $\mathbb{T}_a f(x) = f(x + a)$ . Combining this feature with the early-time expansion of the heat-kernel on the sphere (A.4), the trace can be rewritten in terms of the Q-functionals defined in (A.7)

$$\mathrm{Tr}_{(s)} [W(\square)] = \frac{1}{(4\pi)^2} \int d^4x \sqrt{g} \sum_{n \geq 0} Q_{2-n} [\mathbb{T}_{E_{(s)}} W] b_n^{(s)} \bar{R}^n. \quad (72)$$

The coefficients  $b_n^{(s)}$  in this expansion can be obtained by summing the eigenvalues of the Laplace-operator on the sphere and are listed in Table A.5 of Appendix Appendix A. For  $d = 4$  the index of the Q-functionals is integer. In this case the  $Q_m$  are related to the function  $W$  via eq. (A.8).

The last missing ingredient in writing down the PDE governing the scale-dependence of  $f_k(R)$  is the specification of the regulator  $R_k$ . Following the previous section, we will again adopt the optimized cutoff (58). This choice has the advantage that only a finite number of terms in the expansion (72) actually contribute to the RG flow [22, 23, 24]. This can be seen as follows. For the specific choice of regulator, the arguments of the Q-functionals appearing in (72) are of the form

$$\mathbb{T}_{E_{(s)}} W_s(z) = [A(z + E_{(s)})^2 + B(z + E_{(s)}) + C] \theta(k^2 - E_s - z). \quad (73)$$

The coefficients  $A$ ,  $B$  and  $C$  depend on the scalar curvature and are independent of  $z$ . For negative index, the Q-functionals are given by derivatives of this function, evaluated at  $z = 0$ . Owing to the polynomial form, only the first two derivatives are contributing to the flow; derivatives acting on  $\theta(k^2 - E_{(s)} - z)$  produce (derivatives of)  $\delta$ -distributions,  $\delta^{(m)}(k^2 - E_{(s)})$ , which are outside the truncation subspace. Thus the traces (70) receive contributions from  $Q_n[\mathbb{T}_{E_{(s)}} W]$ ,  $n \geq -2$ , only.

At this stage, we have all ingredients to explicitly compute the two traces (70). In order to write the result in a compact form, we specify the endomorphisms as

$$E_{(2)} = \alpha \bar{R}, \quad E_{(0)} = \beta \bar{R}. \quad (74)$$

Denoting the derivative of  $f_k(\bar{R})$  with respect to  $\bar{R}$  by a prime and its  $t$ -derivative with a dot, the result for the traces then reads

$$\begin{aligned} T_{(0)} &= \frac{k^6}{16\pi^2} \frac{384\pi^2}{\bar{R}^2} \frac{c_1 f' + c_2 k^2 f'' + c_3 \dot{f}' + c_4 k^2 \dot{f}''}{(3k^2 - (3\beta + 1)\bar{R})^2 f'' + (3k^2 - (3\beta + 2)\bar{R}) f' + 2f}, \\ T_{(2)} &= \frac{k^6}{16\pi^2} \frac{384\pi^2}{\bar{R}^2} \frac{\tilde{c}_1 f' + \tilde{c}_2 \dot{f}'}{(3k^2 - (3\alpha + 1)\bar{R}) f' + 3f}. \end{aligned} \quad (75)$$

The coefficients are conveniently be expressed in terms of the dimensionless curvature  $r \equiv \bar{R}k^{-2}$  and read

$$\begin{aligned}
c_1 &= 3 + (1 - 6\beta)r + \frac{1080\beta^2 - 360\beta + 29}{360} r^2, \\
c_2 &= 18 - 54\beta r + \frac{3240\beta^2 - 91}{60} r^2 - \frac{3240\beta^3 - 273\beta + 29}{180} r^3, \\
c_3 &= \frac{1}{2} + \frac{1-6\beta}{4} r + \frac{1080\beta^2 - 360\beta + 29}{720} r^2 - \frac{45360\beta^3 - 22680\beta^2 + 3654\beta - 185}{90720} r^3, \\
c_4 &= \frac{9}{4} - 9\beta r + \frac{3240\beta^2 - 91}{240} r^2 - \frac{3240\beta^3 - 273\beta + 29}{360} r^3 + \\
&\quad + \frac{90720\beta^4 - 15288\beta^2 + 3248\beta - 181}{40320} r^4.
\end{aligned} \tag{76}$$

and

$$\begin{aligned}
\tilde{c}_1 &= 15 - (30\alpha + 5)r + \frac{1080\alpha^2 + 360\alpha - 1}{72} r^2, \\
\tilde{c}_2 &= \frac{5}{2} - \frac{30\alpha + 5}{4} r + \frac{1080\alpha^2 + 360\alpha - 1}{144} r^2 - \frac{45360\alpha^3 + 22680\alpha^2 - 126\alpha - 311}{18144} r^3.
\end{aligned} \tag{77}$$

The PDE governing the scale-dependence of  $f_k(R)$  is then obtained by substituting eqs. (64) and (75) into (46). It is most conveniently expressed in terms of the dimensionless quantities

$$r \equiv \bar{R}k^{-2}, \quad f_k(R) \equiv k^4 \varphi_k(\bar{R}k^{-2}). \tag{78}$$

In terms of these, the flow becomes

$$\begin{aligned}
32\pi^2 (\dot{\varphi} + 4\varphi - 2r\varphi') &= \frac{(\tilde{c}_1 + 2\tilde{c}_2) \varphi' + \tilde{c}_2 (\dot{\varphi}' - 2r\varphi'')}{(3 - (3\alpha + 1)r) \varphi' + 3\varphi} \\
&\quad + \frac{d_1 \varphi' + d_2 \varphi'' + c_3 \dot{\varphi}' + c_4 (\dot{\varphi}'' - 2r\varphi''')}{(3 - (3\beta + 1)r)^2 \varphi'' + (3 - (3\beta + 2)r) \varphi' + 2\varphi},
\end{aligned} \tag{79}$$

with  $d_1 = c_1 + 2c_3$  and  $d_2 = c_2 - 2rc_3$ . Again, it is implicitly understood that  $\varphi \equiv \varphi_k(r)$  and primes denote derivatives with respect to  $r$  while the dots are derivatives with respect to the renormalization group time  $t = \ln(k)$ . The polynomials  $c_i$  and  $\tilde{c}_i$  given in eqs. (76) and (77), respectively. Since the flow equation has been derived on a spherical background with  $\bar{R} > 0$ , it is valid for  $r \geq 0$ . Eq. (79) constitutes the central result of this section.

## 5. The $f(R)$ -truncation: properties of the RG flow

We now proceed by analyzing the properties of the PDE (79), governing the scale-dependence of the dimensionless function  $\varphi_k(r)$  by projecting the PDE onto the subspace spanned by polynomials of the curvature scalar and explore the resulting fixed point structure. In this way, we identify the

NGFP generalizing the Einstein-Hilbert analysis (cf. Tab. 1). The properties of the NGFP then depend on the endomorphisms introduced in the regularization procedure. This dependence is studied in detail and minimized following the principle of minimum sensitivity (PMS), “optimizing” the value of the critical exponents found within a given truncation.

In order to get a more profound picture of the fixed point structure entailed by the PDE (79), we resort to a polynomial ansatz for  $\varphi_k(r)$ , including powers of the dimensionless curvature up to  $r^N$

$$\varphi_k(r) = \sum_{m=0}^N g_m r^m, \quad \partial_t \varphi_k(r) = \sum_{m=0}^N \beta_{g_m} r^m. \quad (80)$$

Here  $g_m$  are the  $k$ -dependent running couplings and  $\beta_{g_m} \equiv \partial_t g_m$  denotes their beta functions. Substituting (80) into (79) and expanding the result in powers of  $r$  up to order  $N$  yields a system of  $N + 1$  algebraic equations which can be solved for the beta functions

$$\beta_{g_m} = \beta_{g_m}(\{g_j\}, \alpha, \beta). \quad (81)$$

The beta functions depend on the couplings  $g_m$  and, owed to the inclusion of the endomorphisms in the regulators, have a parametric dependence on  $\alpha, \beta$ . At a fixed point of the RG flow  $g_m^*$ , the beta functions (81) vanish. Owed to the parametric dependence on  $\alpha, \beta$  the position of such a fixed point  $g_m^*(\alpha, \beta)$  and its stability coefficients  $\theta_m(\alpha, \beta)$  (defined as minus the eigenvalues of the stability matrix (61)) depend on the endomorphisms.

We now extend our analysis of the NGFP identified in Sect. 3 to the polynomial truncations (80). This extension has to be carried out with care, since new, unphysical fixed points appear, when increasing the order  $N$  of the expansion. Thus, it is necessary to identify the correct NGFP at low order ( $N = 1$ ) and increase the dimension of the truncation step by step. By comparing the values of the fixed points at the order  $N$  with those determined at the previous order  $N - 1$ , it is possible to trace the NGFP through the system (80).

In order to make contact with previous works and the Einstein-Hilbert truncation of Sect. 3, we first study the system (81) for vanishing endomorphisms ( $\alpha = \beta = 0$ ). The position of the NGFP for the orders  $N = 1$  to  $N = 6$  are summarized in the first block of Tab. 2. Notably, the NGFP exists for all values  $N$  and its position converges rapidly when increasing the size of the truncation  $N$ . The critical exponents of the NGFP obtained by evaluating (61) are given in the first block Tab. 3. Again we observe a rapid convergence of the critical exponents with increasing value  $N$ . Moreover, extending the system beyond  $N > 2$  does not give rise to further relevant deformations, characterized by  $\text{Re}\theta > 0$ : the number of relevant deformations stabilizes at three. This is a strong indication that classical power counting still constitutes a good ordering principle for the relevance

| $N$ | $g_0^*$ | $g_1^*$ | $g_2^*$ | $g_3^*$ | $g_4^*$ | $g_5^*$ | $g_6^*$ |
|-----|---------|---------|---------|---------|---------|---------|---------|
| 1   | 0.0103  | -0.0255 |         |         |         |         |         |
| 2   | 0.0105  | -0.0225 | 0.0025  |         |         |         |         |
| 3   | 0.0105  | -0.0242 | 0.0022  | -0.0086 |         |         |         |
| 4   | 0.0102  | -0.0246 | 0.0020  | -0.0095 | -0.0085 |         |         |
| 5   | 0.0102  | -0.0247 | 0.0020  | -0.0083 | -0.0083 | -0.0053 |         |
| 6   | 0.0102  | -0.0247 | 0.0020  | -0.0083 | -0.0082 | -0.0053 | -0.0002 |
| 1   | 0.0110  | -0.0248 |         |         |         |         |         |
| 2   | 0.0116  | -0.0235 | 0.0026  |         |         |         |         |
| 3   | 0.0112  | -0.0237 | 0.0024  | -0.0145 |         |         |         |
| 4   | 0.0111  | -0.0238 | 0.0024  | -0.0146 | -0.0073 |         |         |
| 5   | 0.0111  | -0.0237 | 0.0024  | -0.0141 | -0.0068 | -0.0046 |         |
| 6   | 0.0111  | -0.0237 | 0.0024  | -0.0141 | -0.0070 | -0.0048 | 0.0013  |
| 1   | 0.0170  | -0.0250 |         |         |         |         |         |
| 2   | 0.0117  | -0.0237 | 0.0026  |         |         |         |         |
| 3   | 0.0110  | -0.0238 | 0.0023  | -0.0121 |         |         |         |
| 4   | 0.0108  | -0.0240 | 0.0023  | -0.0125 | -0.0077 |         |         |
| 5   | 0.0108  | -0.0240 | 0.0023  | -0.0119 | -0.0074 | -0.0046 |         |
| 6   | 0.0108  | -0.0240 | 0.0023  | -0.0119 | -0.0078 | -0.0047 | 0.0016  |

Table 2: Position of the NGFP in the polynomial expansion for the equation with  $\alpha = 0$  and  $\beta = 0$  (upper box), the equal lowest eigenvalue condition with  $\beta = 1/6, \alpha = -1/2$  (middle box), and for the choice of endomorphisms (83) favored by the principle of minimum sensitivity (lower box).

of operators at the NGFP. Operators which are power-counting irrelevant at the classical level do not correspond to relevant deformations at the NGFP. All these findings are in complete agreement with earlier studies based on non-geometric flow equations [23, 24]. It is quite remarkable, however, that for  $N = 2$  the critical exponent  $\theta_2$  is much closer to the values found for  $N > 2$ , indicating that the geometric flows studied here are less sensitive to such outliers.

Based on the confidence obtained from the flow equation with  $\alpha = \beta = 0$ , we now carry out a systematic analysis on the influence of the endomorphisms. Since  $\alpha$  and  $\beta$  have been introduced via the cutoff functions, the variation of these parameters corresponds to a change in the regularization procedure. Naturally, potential observables should not depend too strongly on the regularization scheme. Therefore the dependence of the beta functions on  $\alpha$  and  $\beta$  may be exploited to optimize the value of the critical exponents obtained within a given truncation by minimizing their dependence on  $\alpha$  and  $\beta$ . This logic follows the principle of minimal sensitivity (PMS).

In practice, we implement this PMS as follows. First we choose the set

| $N$ | $\theta_0$        | $\theta_1$ | $\theta_2$          | $\theta_3$ | $\theta_4$ | $\theta_5$ | $\theta_7$ |
|-----|-------------------|------------|---------------------|------------|------------|------------|------------|
| 1   | $2.93 \pm 2.97_1$ |            |                     |            |            |            |            |
| 2   | $2.69 \pm 4.61_1$ | 8.72       |                     |            |            |            |            |
| 3   | $3.24 \pm 3.10_1$ | 1.79       | -8.09               |            |            |            |            |
| 4   | $3.43 \pm 3.14_1$ | 1.53       | $-6.45 \pm 2.92_1$  |            |            |            |            |
| 5   | $3.41 \pm 3.33_1$ | 1.55       | $-4.03 \pm 8.12_1$  |            |            | -5.03      |            |
| 6   | $3.08 \pm 3.17_1$ | 1.52       | $-2.78 \pm 11.21_1$ |            |            | -4.86      | -10.84     |
| 1   | $3.06 \pm 3.73_1$ |            |                     |            |            |            |            |
| 2   | $3.01 \pm 6.87_1$ | 4.86       |                     |            |            |            |            |
| 3   | $3.42 \pm 4.07_1$ | 1.71       | -10.08              |            |            |            |            |
| 4   | $3.68 \pm 4.22_1$ | 1.66       | $-9.60 \pm 3.13_1$  |            |            |            |            |
| 5   | $3.59 \pm 4.30_1$ | 1.68       | $-6.36 \pm 14.43_1$ |            |            | -5.70      |            |
| 6   | $3.51 \pm 4.25_1$ | 1.80       | $-3.76 \pm 16.33_1$ |            |            | -5.61      | -13.73     |
| 1   | $3.00 \pm 3.42_1$ |            |                     |            |            |            |            |
| 2   | $2.47 \pm 5.93_1$ | 4.74       |                     |            |            |            |            |
| 3   | $3.35 \pm 3.73_1$ | 1.67       | -9.42               |            |            |            |            |
| 4   | $3.59 \pm 3.83_1$ | 1.61       | $-7.50 \pm 4.10_1$  |            |            |            |            |
| 5   | $3.54 \pm 3.96_1$ | 1.63       | $-4.58 \pm 10.95_1$ |            |            | -5.78      |            |
| 6   | $3.40 \pm 3.90_1$ | 1.61       | $-2.40 \pm 11.85_1$ |            |            | -5.67      | -12.14     |

Table 3: Stability coefficients associated with the NGFP identified in Tab. 2 with  $\alpha = 0$  and  $\beta = 0$  (upper box), the equal lowest eigenvalue condition with  $\beta = 1/6, \alpha = -1/2$  (middle box), and for the choice of endomorphisms (83) favored by the principle of minimum sensitivity (lower box).

of observables whose regulator-dependence should be minimized. We pick the real part of the relevant stability coefficients,  $\text{Re}\theta_1$  and  $\theta_2$  as well as the “universal product” [15]

$$\tau_* \equiv g_* \lambda_* = \frac{g_0^*}{32 \pi (g_1^*)^2}. \quad (82)$$

Subsequently, we expand  $\varphi_k(r)$  to the order  $N = 3$  and compute these quantities as functions of  $\alpha$  and  $\beta$ . In the first analysis we confine ourselves to a one dimensional subspace of regulators obeying the condition of equal lowest eigenvalues (67) by setting  $\alpha = \beta - \frac{2}{3}$ . The values of  $\text{Re}\theta_1$ ,  $\theta_2$  and  $\tau_*$  along this line are displayed in Fig. 2. While  $\text{Re}\theta_1$  and  $\tau_*$  show a monotonic behavior,  $\theta_2(\beta)$  shows a minimum at

$$\beta \approx 0.332683, \quad \alpha \approx -0.333984. \quad (83)$$

The value of  $\tau_*$  decreases mildly with growing  $\beta$ . The range of values  $0.175 \geq \tau_* \geq 0.2$  found in the linear-geometric case is similar to the values for  $\tau_*$  found within previous non-geometric studies [15, 24], adding further confidence to the linear-geometric approximation.

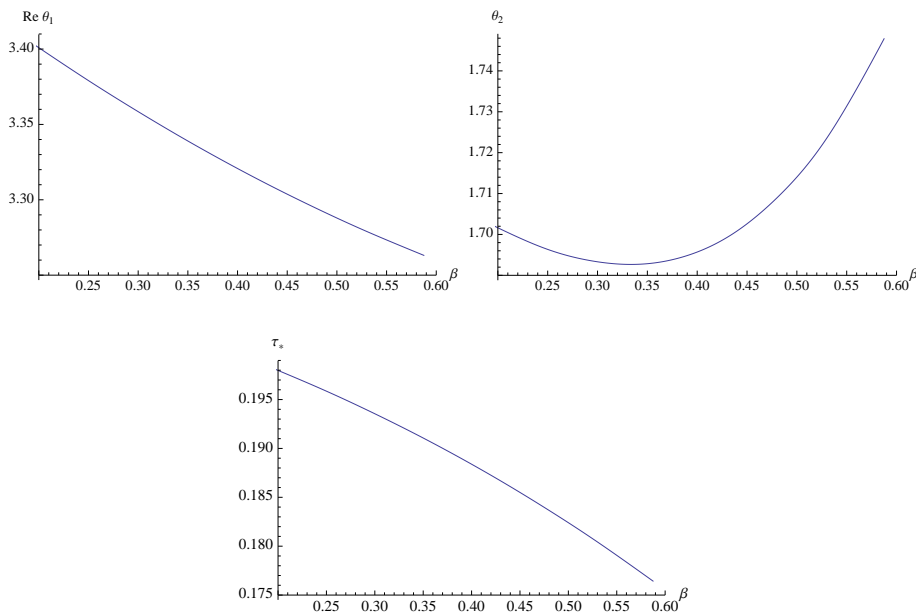


Figure 2: Stability coefficients  $\text{Re } \theta_1$ ,  $\theta_2$  and  $\tau_*$  as a function of the endomorphisms  $\alpha$  and  $\beta$  along the line of equal lowest eigenvalues  $\alpha = \beta - \frac{2}{3}$ .

Now that we have identified a preferred choice for the endomorphisms, we repeat our fixed point study for the distinguished choice (83). The position of the NGFP  $g_m^*$  and its critical exponents  $\theta_m$  are shown in the lower boxes of Tab. 2 and Tab. 3, respectively. Comparing the upper and lower parts of the tables establishes that the NGFP and its properties display a weak dependence on the endomorphisms only: the optimized values differ very little from the  $\alpha = \beta = 0$  case. Thus the polynomial  $f(R)$ -computation shows a strong robustness with respect to varying the regulator functions. Moreover, the PMS choice (83) significantly reduces the outlier  $\theta_2$  found for  $N = 2$  (reported to be  $8.4 \leq \theta_2 \leq 28.8$  in [20]) is further decreased, so that its value is only one fifth of the one found in non-geometric computations [23, 24]. This analysis indicates that the Type I regularization procedure corresponding to vanishing endomorphisms ( $\alpha = \beta = 0$ ), is actually not favored by PMS: including a non-trivial endomorphism reduces the dependence of observables on the regulator and improves the convergence properties of the polynomial truncations.

## 6. Summary and Outlook

We proposed a novel renormalization group equation for Quantum Einstein Gravity (QEG) of geometric type. The construction involves a reference background, over which fluctuations of the metric are integrated out

following the ideas of the Wilsonian renormalization group (RG). The geometric setting eliminates redundant gauge configurations through an opportune choice of coordinates on the configuration space: the coordinates are adapted to the fiber-bundle structure and the gauge degrees of freedom are removed by restricting the integration measure to the base space. Consequently, the flow equation is formulated in terms of fluctuation fields, which are invariant with respect to quantum gauge transformations and transform covariantly with respect to background gauge transformations. The resulting flow is manifestly invariant under both symmetries and all expectation values are gauge invariant by construction. Both the original Wetterich-type flow equations for gravity [8, 15] and the geometric flow equation constructed in this paper are exact functional renormalization group equations for QEG, which allow for the exploration of the theory’s RG flow away from the Gaussian fixed point. The structure of the geometrical flow equation is considerably simpler, however, since there are no contributions from the gauge degrees of freedom, ghost fields and auxiliary fields encoding the Jacobians of the TT-decomposition.

In order to be able to perform explicit computations, we chose a generic background metric as the base point and decomposed the fluctuations via a transverse-traceless decomposition with respect to this background. Subsequently, we approximated the exact geometric flow by truncating the map between fluctuations and gauge-invariant fields at the linear level. In this “linear geometric approximation”, the gauge-invariant fields of the geometric construction coincide with those of the transverse-traceless decomposition. From a geometric viewpoint, this approximation neglects the contributions coming from the Vilkovisky-De Witt connection of the geometric formalism, that appears upon projecting the redundant configuration space of the fields onto the space of physically distinguished configurations. The flow obtained in this way is driven by quantum fluctuations of the transverse-traceless and trace part of the fluctuation field and agrees with the functional renormalization group equation [8] for a specific choice of regulator function and gauge.

In this work we have performed a first set of non-trivial tests of the Asymptotic Safety conjecture based on the linearized geometric approximation. At the level of the four-dimensional Einstein-Hilbert truncation the standard phase diagram of QEG [16] is recovered and the critical exponents associated with the non-Gaussian fixed point (NGFP) controlling the UV-behavior of the theory, turn out quantitatively similar. Our results can also be analytically continued in the dimensionality of the system, allowing to explore all dimensionalities and follow the NGFP up to the upper critical dimension of gravity. Notably, the geometric beta functions possess a discontinuity when approaching the lower critical dimension,  $d = 2$ , which is related to the fact that there are no transverse-traceless tensors on a two-dimensional sphere.

One of the key advantages of the geometric flow equation becomes apparent at the level of functional truncation including an infinite number of coupling constants. Constructing the partial differential equation (PDE) that governs the RG flow of the function  $f_k(R)$ , the absence of gauge degrees of freedom, ghosts, and auxiliary fields implies that the singularity structure of the PDE is completely determined by the contributions of the (approximately) gauge-invariant fields. As it will turn out [78], the resulting structure is precisely the one needed for obtaining isolated and globally well-defined fixed functionals.

For the purpose of this work, however, we limited ourselves to a RG flow study performing a polynomial expansion of  $f_k(R)$  which incorporates higher powers of the Ricci scalar in the truncation ansatz. As a novel feature, our construction of the beta functions includes a non-trivial endomorphism in the regularization procedure. Systematically increasing the order of the polynomial reliably identifies a unique NGFP. Including an increasing number of power-counting irrelevant operators, we establish that the fixed point comes with three relevant deformations. Its position and critical exponents are in good agreement with earlier studies based on the non-geometric constructions [22, 23, 24, 96]. The finite (non-increasing) number of relevant deformations in the geometric flow equation is another signal underpinning the predictivity of Asymptotic Safety. Moreover, the coherence with earlier findings also corroborates the validity of our construction.

Notably, the properties of the NGFP show very little sensitivity towards the change of the regularization procedure. The parametric dependence of the beta functions on the endomorphisms allows to apply the principle of minimal sensitivity to the stability coefficients of the NGFP. This principle allows to determine what set of parameters is numerically preferred by minimizing the highest real critical exponent of the NGFP, meaning that the system converges more rapidly to its critical point in a statistical mechanical sense [77]. The results become thus more reliable because it can be argued that there is less sensitivity on the operators that are neglected from the projection procedure. Interestingly, this work shows that a regulator that utilizes operators with non-zero endomorphisms (Type II cutoffs in the language of [24]) is preferred over a regularization procedure based on Laplacian operators only (Type I cutoff).

Clearly, the geometrical flow equation may play an important role when computing vacuum expectation values of gauge-invariant combinations of the fluctuation fields. Moreover, keeping track of the fluctuation fields (so-called bi-metric computations) may be carried out more economically, especially when exploiting the Ward identities of the construction [18, 86]. Thus the geometric flow equation may be helpful in understanding the actual driving elements of the gravitational RG flow, which might have been previously overshadowed by gauge-effects. In order to perform such computations, it is clear that the natural generalization of the method adopted in this pa-

per is to take into account the non-vanishing curvature of the fiber-bundle structure underlying the gravitational configuration space. This requires the knowledge of the map (29) at least to quadratic order, while the computation of gauge-invariant vacuum expectation values of the fluctuation fields will require going beyond the quadratic approximation. We hope to come back to this point in the future.

## Acknowledgments

We thank A. Nink and M. Reuter for many helpful discussions. The research of F. S. and O. Z. has been supported by the Deutsche Forschungsgemeinschaft (DFG) within the Emmy-Noether program (Grant SA/1975 1-1).

## Appendix A. The heat-kernel on the $d$ -sphere $S^d$

The explicit computation of the gravitational beta functions requires the evaluation of the functional traces appearing on the r.h.s. of the flow equation (18). These calculations are conveniently done by applying results for the heat-kernel on a  $d$ -sphere and we collect the relevant formulas in this appendix.

### Appendix A.1. Heat-kernel on $S^d$ : early time expansion

Throughout this paper we chose the background metric  $\bar{g}_{\mu\nu}$  to be the one of the  $d$ -dimensional sphere. This implies that the curvature tensors constructed from  $\bar{g}_{\mu\nu}$  satisfy

$$\bar{R}_{\mu\nu\rho\sigma} = \frac{\bar{R}}{d(d-1)} (\bar{g}_{\mu\rho} \bar{g}_{\nu\sigma} - \bar{g}_{\mu\sigma} \bar{g}_{\nu\rho}) , \quad \bar{R}_{\mu\nu} = \frac{1}{d} \bar{g}_{\mu\nu} \bar{R} , \quad (\text{A.1})$$

and are covariantly constant. Moreover, the volume of the  $d$ -sphere is related to the Ricci scalar by

$$\text{Vol}_{S^d} \equiv \int_{S^d} d^d x \sqrt{\bar{g}} = \frac{\Gamma(d/2)}{\Gamma(d)} \left( \frac{4\pi d(d-1)}{\bar{R}} \right)^{d/2} . \quad (\text{A.2})$$

The fact that the background curvatures are covariantly constant allows to relate a function  $W(x)$  depending on the covariant background Laplacian  $\Delta \equiv -\bar{g}^{\mu\nu} \bar{D}_\mu \bar{D}_\nu$  to the heat-kernel of  $\Delta$  in a rather simple way

$$\text{Tr}_{(s)} [W(\Delta)] = \int_0^\infty d\sigma \widetilde{W}(\sigma) \text{Tr}_{(s)} [e^{-\sigma\Delta}] . \quad (\text{A.3})$$

Here  $\widetilde{W}$  is the inverse Laplace transform of  $W$  and the subscript  $(s)$  on the traces indicates whether  $\Delta$  acts on symmetric transverse traceless tensors

( $s = 2$ ), transverse vectors ( $s = 1$ ), or scalars ( $s = 0$ ). The heat trace admits an early-time expansion

$$\mathrm{Tr}_{(s)} [e^{-\sigma\Delta}] \simeq \frac{1}{(4\pi\sigma)^{d/2}} \int_{S^d} d^d x \sqrt{\bar{g}} \sum_{n \geq 0} b_n^{(s)} \sigma^n \bar{R}^n. \quad (\text{A.4})$$

The expansion coefficients  $b_n^{(s)}$  depend on the spin of the field. Following ref. [15] they can be obtained from the early-time expansion of tensor fields without differential constraints. The first two coefficients obtained in this way are

$$\begin{aligned} b_0^{(0)} &= 1, & b_1^{(0)} &= \frac{1}{6}, \\ b_0^{(2)} &= \frac{(d-2)(d+1)}{2}, & b_1^{(2)} &= \frac{(d+1)(d+2)(d-5+3\delta_{d,2})}{12(d-1)}. \end{aligned} \quad (\text{A.5})$$

Substituting (A.4) into (A.3), the operator trace can be written as

$$\mathrm{Tr}_{(s)} [W(\Delta)] = \frac{1}{(4\pi)^{d/2}} \int d^d x \sqrt{\bar{g}} \sum_{n \geq 0} Q_{d/2-n}[W] b_n^{(s)} \bar{R}^n, \quad (\text{A.6})$$

with the  $Q$ -functionals defined as

$$Q_n[W] \equiv \int_0^\infty d\sigma \sigma^{-n} \widetilde{W}(\sigma) \quad (\text{A.7})$$

For  $n > 0$  this definition can be related to  $W$  by a Mellin-transform

$$\begin{aligned} Q_n[W] &= \frac{1}{\Gamma(n)} \int_0^\infty dz z^{n-1} W(z), & n &> 0, \\ Q_{-m}[W] &= (-1)^m W^{(m)}(0), & m &\geq 0 \in \mathbb{N}, \end{aligned} \quad (\text{A.8})$$

with  $W^{(m)}(z)$  denoting the  $m$ th derivative of  $W$  with respect to the argument. Based on these formulas, the derivation of the beta functions (53) is rather straightforward.

#### *Appendix A.2. Heat-kernel on $S^4$ : the asymptotic series*

The derivation of the PDE governing the scale-dependence of  $f_k(R)$  in Sect. 4 requires knowing the expansion coefficients  $b_n^{(s)}$  for  $s = 0, 2$  to higher order in  $n$ . The coefficients can be found by relating the heat kernel to the sum over eigenvalues  $\lambda_l(d, s)$  of the operator  $\Delta$  weighted by their multiplicity  $M_l(d, s)$

$$\mathrm{Tr}_{(s)} [e^{-\sigma\Delta}] = \sum_l M_l(d, s) e^{-\sigma\lambda_l(d, s)}. \quad (\text{A.9})$$

| Spin $s$ | Eigenvalue $\lambda_l(d, s)$  | Multiplicity $M_l(d, s)$                                     |                   |
|----------|-------------------------------|--|-------------------|
| 0        | $\frac{l(l+d-1)}{d(d-1)} R$   | $\frac{(2l+d-1)(l+d-2)!}{l!(d-1)!}$                          | $l = 0, 1, \dots$ |
| 2        | $\frac{l(l+d-1)-2}{d(d-1)} R$ | $\frac{(d-2)(d+1)(l-1)(d+l)(d+2l-1)(d+l-3)!}{2(d-1)!(l+1)!}$ | $l = 2, 3, \dots$ |

Table A.4: Eigenvalues  $\lambda_l(d, s)$  and multiplicities  $M_l(d, s)$  of the Laplacian operator  $\Delta \equiv -D^2$  acting on fields with spin  $s$  on the  $d$ -sphere [97, 98].

For general  $d$ ,  $\lambda_l(d, s)$  and  $M_l(d, s)$  have been computed in [97, 98] and are listed in Tab. A.4. We stress that for  $d$  even, (A.9) only constitutes an asymptotic series [99]. The first two terms in the expansion are universal while the coefficients multiplying higher powers of  $R$  may depend on the resummation scheme. We fix this freedom by demanding that (A.9) reproduces the early-time expansion (A.4) evaluated on the  $d$ -sphere.

The case where (A.9) reproduces the early-time expansion of the heat kernel evaluates the sum using the Euler-MacLaurin formula

$$\sum_{n=a}^b f(n) \sim \int_a^b f(x) dx + \frac{f(b) + f(a)}{2} + \sum_{k=1}^{\infty} \frac{B_{2k}}{(2k)!} \left( f^{(2k-1)}(b) - f^{(2k-1)}(a) \right). \quad (\text{A.10})$$

Here  $B_{2k}$  denotes the Bernoulli numbers. For  $d = 4$  the functions  $f^{(s)}(x)$  entering into (A.10) are

$$\begin{aligned} f^{(0)}(x) &= \frac{1}{6}(x+1)(x+2)(2x+3)e^{-\frac{1}{12}x(x+3)R\sigma}, \\ f^{(2)}(x) &= \frac{5}{6}(x-1)(x+4)(2x+3)e^{-\frac{1}{12}(x(x+3)-2)R\sigma}, \end{aligned} \quad (\text{A.11})$$

with boundaries  $a = 0, b = \infty$  ( $s = 0$ ) and  $a = 2, b = \infty$  ( $s = 2$ ). The integral parts in (A.10) are then given by

$$\begin{aligned} \int_0^{\infty} dx f^{(0)}(x) &= \frac{1}{(4\pi\sigma)^2} \int_{S^d} d^d x \sqrt{g} \left( 1 + \frac{1}{6}\sigma\bar{R} \right), \\ \int_2^{\infty} dx f^{(2)}(x) &= \frac{1}{(4\pi\sigma)^2} \int_{S^d} d^d x \sqrt{g} \left( 5 + \frac{5}{2}\sigma\bar{R} \right) e^{-\frac{2\bar{R}\sigma}{3}} \end{aligned} \quad (\text{A.12})$$

where we have reinstalled the volume integral via the relation (A.2). In contrast to the scalar case, where the integral part determines the first two heat-kernel coefficients, the integral for  $s = 2$  contributes to all orders in  $\bar{R}$ . The sums in (A.10) start contributing at order  $\bar{R}^2$  in the expansion and the corresponding coefficients can be computed by evaluating them on a term by term basis truncating the infinite sufficiently high order. This procedure yields the heat-kernel coefficients  $b_n^{(s)}$  listed in Tab. A.5. These coefficients form the basis for constructing the PDE governing the scale-dependence of  $f_k(R)$  in Sect. 4.

| s | $b_0^{(s)}$ | $b_1^{(s)}$    | $b_2^{(s)}$       | $b_3^{(s)}$         | $b_4^{(s)}$           | $b_5^{(s)}$             |
|---|-------------|----------------|-------------------|---------------------|-----------------------|-------------------------|
| 0 | 1           | $\frac{1}{6}$  | $\frac{29}{2160}$ | $\frac{37}{54432}$  | $\frac{149}{6531840}$ | $\frac{179}{431101440}$ |
| 2 | 5           | $-\frac{5}{6}$ | $-\frac{1}{432}$  | $\frac{311}{54432}$ | $\frac{109}{1306368}$ | $-\frac{317}{12317184}$ |

Table A.5: Heat kernel coefficients appearing in the early-time expansion of (A.4) on the four-sphere.

## References

- [1] S. Weinberg in *General Relativity, an Einstein Centenary Survey*, S.W. Hawking and W. Israel (Eds.), Cambridge University Press, 1979; S. Weinberg, hep-th/9702027.
- [2] S. Weinberg, arXiv:0903.0568.
- [3] S. Weinberg, PoS C D09 (2009) 001, arXiv:0908.1964.
- [4] M. Niedermaier and M. Reuter, Living Rev. Rel. **9** (2006) 5.
- [5] M. Reuter and F. Saueressig, in *Geometric and Topological Methods for Quantum Field Theory*, H. Ocampo, S. Paycha and A. Vargas (Eds.), Cambridge University Press, Cambridge, 2010, arXiv:0708.1317.
- [6] R. Percacci, in *Approaches to Quantum Gravity: Towards a New Understanding of Space, Time and Matter*, D. Oriti (Ed.), Cambridge University Press, Cambridge, 2009, arXiv:0709.3851.
- [7] M. Reuter and F. Saueressig, New J. Phys. **14** (2012) 055022, arXiv:1202.2274.
- [8] M. Reuter, Phys. Rev. D **57** (1998) 971, hep-th/9605030.
- [9] C. Wetterich, Phys. Lett. B **301** (1993) 90.
- [10] T. R. Morris, Int. J. Mod. Phys. A **9** (1994) 2411, hep-ph/9308265.
- [11] D. F. Litim and J. M. Pawłowski, Phys. Rev. D **66** (2002) 025030, hep-th/0202188.
- [12] A. Codello, M. Demmel and O. Zanusso, Phys. Rev. D **90** (2014) 027701, arXiv:1310.7625.
- [13] D. Dou and R. Percacci, Class. Quant. Grav. **15** (1998) 3449, hep-th/9707239.
- [14] W. Souma, Prog. Theor. Phys. **102** (1999) 181, hep-th/9907027.

- [15] O. Lauscher and M. Reuter, Phys. Rev. D **65** (2002) 025013, hep-th/0108040.
- [16] M. Reuter and F. Saueressig, Phys. Rev. D **65** (2002) 065016, hep-th/0110054.
- [17] S. Nagy, J. Krizsan and K. Sailer, JHEP **07** (2012) 102, arXiv:1203.6564.
- [18] I. Donkin and J. M. Pawłowski, arXiv:1203.4207.
- [19] O. Lauscher and M. Reuter, Class. Quant. Grav. **19** (2002) 483, hep-th/0110021.
- [20] O. Lauscher and M. Reuter, Phys. Rev. D **66** (2002) 025026, hep-th/0205062.
- [21] S. Rechenberger and F. Saueressig, Phys. Rev. D **86** (2012) 024018, arXiv:1206.0657.
- [22] A. Codello, R. Percacci and C. Rahmede, Int. J. Mod. Phys. A **23** (2008) 143, arXiv:0705.1769.
- [23] P. F. Machado and F. Saueressig, Phys. Rev. D **77** (2008) 124045, arXiv:0712.0445.
- [24] A. Codello, R. Percacci and C. Rahmede, Annals Phys. **324** (2009) 414, arXiv:0805.2909.
- [25] A. Bonanno, A. Contillo and R. Percacci, Class. Quant. Grav. **28** (2011) 145026, arXiv:1006.0192.
- [26] C. Rahmede, PoS CLAQG **08** (2011) 011.
- [27] K. Falls, D. F. Litim, K. Nikolakopoulos and C. Rahmede, arXiv:1301.4191.
- [28] D. Benedetti, P. F. Machado and F. Saueressig, Mod. Phys. Lett. A **24** (2009) 2233, arXiv:0901.2984.
- [29] D. Benedetti, P. F. Machado and F. Saueressig, Nucl. Phys. B **824** (2010) 168, arXiv:0902.4630.
- [30] D. Becker and M. Reuter, JHEP **07** (2012) 172, arXiv:1205.3583.
- [31] A. Eichhorn, H. Gies and M. M. Scherer, Phys. Rev. D **80** (2009) 104003, arXiv:0907.1828.
- [32] K. Groh and F. Saueressig, J. Phys. A **43** (2010) 365403, arXiv:1001.5032.

- [33] A. Eichhorn and H. Gies, Phys. Rev. D **81** (2010) 104010, arXiv:1001.5033.
- [34] D. Benedetti, Europhys. Lett. **102** (2013) 20007, arXiv:1301.4422.
- [35] P. Fischer and D. F. Litim, AIP Conf. Proc. **861** (2006) 336, hep-th/0606135.
- [36] N. Ohta, Class. Quant. Grav. **29** (2012) 205012, arXiv:1205.0476.
- [37] M. Reuter and H. Weyer, Phys. Rev. D **79** (2009) 105005, arXiv:0801.3287.
- [38] M. Reuter and H. Weyer, Phys. Rev. D **80** (2009) 025001, arXiv:0804.1475.
- [39] M. Reuter and H. Weyer, Gen. Rel. Grav. **41** (2009) 983, arXiv:0903.2971.
- [40] P. F. Machado and R. Percacci, Phys. Rev. D **80** (2009) 024020, arXiv:0904.2510.
- [41] A. Bonanno and F. Guarneri, Phys. Rev. D **86** (2012) 105027, arXiv:1206.6531.
- [42] G. 't Hooft, arXiv:1011.0061.
- [43] E. Manrique and M. Reuter, Annals Phys. **325** (2010) 785, arXiv:0907.2617.
- [44] E. Manrique, M. Reuter and F. Saueressig, Annals Phys. **326** (2011) 440, arXiv:1003.5129.
- [45] E. Manrique, M. Reuter and F. Saueressig, Annals Phys. **326** (2011) 463, arXiv:1006.0099.
- [46] D. Becker and M. Reuter, Annals Phys. **350** (2014) 225, arXiv:1404.4537.
- [47] A. Codello, G. D'Odorico and C. Pagani, Phys. Rev. D **89** (2014) 081701, arXiv:1304.4777.
- [48] N. Christiansen, D. F. Litim, J. M. Pawłowski and A. Rodigast, Phys. Lett. B **728** (2014) 114, arXiv:1209.4038.
- [49] N. Christiansen, B. Knorr, J. M. Pawłowski and A. Rodigast, arXiv:1403.1232.
- [50] D. Becker and M. Reuter, arXiv:1412.0468.

- [51] E. Manrique, S. Rechenberger and F. Saueressig, Phys. Rev. Lett. **106** (2011) 251302 arXiv:1102.5012.
- [52] S. Rechenberger and F. Saueressig, JHEP **03** (2013) 010, arXiv:1212.5114.
- [53] P. Hořava, Phys. Rev. D **79** (2009) 084008, arXiv:0901.3775.
- [54] G. D'Odorico, F. Saueressig and M. Schutten, Phys. Rev. Lett. **113** (2014) 171101, arXiv:1406.4366.
- [55] D. Benedetti, K. Groh, P. F. Machado and F. Saueressig, JHEP **06** (2011) 079, arXiv:1012.3081.
- [56] K. Groh, S. Rechenberger, F. Saueressig and O. Zanusso, PoS EPS **-HEP2011** (2011) 124, arXiv:1111.1743.
- [57] K. Groh, F. Saueressig and O. Zanusso, arXiv:1112.4856.
- [58] A. Nink and M. Reuter, JHEP **01** (2013) 062, arXiv:1208.0031.
- [59] U. Harst and M. Reuter, JHEP **05** (2012) 005, arXiv:1203.2158.
- [60] U. Harst and M. Reuter, arXiv:1410.7003.
- [61] A. Contillo, S. Rechenberger and F. Saueressig, JHEP **12** (2013) 017, arXiv:1309.7273.
- [62] R. Loll, Living Rev. Rel. **1** (1998) 13, gr-qc/9805049.
- [63] J. Ambjørn, J. Jurkiewicz and R. Loll, Phys. Rev. Lett. **85** (2000) 924, hep-th/0002050.
- [64] J. Ambjørn, A. Goerlich, J. Jurkiewicz and R. Loll, Phys. Rept. **519** (2012) 127, arXiv:1203.3591.
- [65] J. Ambjørn, J. Jurkiewicz and R. Loll, Phys. Rev. Lett. **93** (2004) 131301, hep-th/0404156.
- [66] J. Ambjørn, J. Jurkiewicz and R. Loll, Phys. Rev. D **72** (2005) 064014, hep-th/0505154.
- [67] J. Ambjørn, S. Jordan, J. Jurkiewicz and R. Loll, Phys. Rev. D **85** (2012) 124044, arXiv:1205.1229.
- [68] J. H. Cooperman, arXiv:1410.0026.
- [69] J. H. Cooperman, arXiv:1406.4531.
- [70] E. Manrique and M. Reuter, Phys. Rev. D **79** (2009) 025008, arXiv:0811.3888.

- [71] M. Reuter and F. Saueressig, JHEP **12** (2011) 012, arXiv:1110.5224.
- [72] J. W. York, J. Math. Phys. **14** (1973) 456.
- [73] J. M. Pawłowski, hep-th/0310018.
- [74] J. M. Pawłowski, Annals Phys. **322** (2007) 2831, hep-th/0512261.
- [75] D. Benedetti, New J. Phys. **14** (2012) 015005, arXiv:1107.3110.
- [76] L. Canet, B. Delamotte, D. Mouhanna and J. Vidal, Phys. Rev. D **67** (2003) 065004, hep-th/0211055.
- [77] L. Canet, B. Delamotte, D. Mouhanna and J. Vidal, Phys. Rev. B **68** (2003) 064421, hep-th/0302227.
- [78] M. Demmel, F. Saueressig and O. Zanusso, in preparation.
- [79] M. Demmel, F. Saueressig and O. Zanusso, JHEP **11** (2012) 131, arXiv:1208.2038.
- [80] M. Demmel, F. Saueressig and O. Zanusso, arXiv:1302.1312.
- [81] M. Demmel, F. Saueressig and O. Zanusso, JHEP **06** (2014) 026, arXiv:1401.5495.
- [82] D. Benedetti and F. Caravelli, JHEP **06** (2012) 017, arXiv:1204.3541.
- [83] D. Benedetti and F. Guarneri, New J. Phys. **16** (2014) 053051, arXiv:1311.1081.
- [84] J. A. Dietz and T. R. Morris, JHEP **01** (2013) 108, arXiv:1211.0955.
- [85] J. A. Dietz and T. R. Morris, JHEP **07** (2013) 064, arXiv:1306.1223.
- [86] I. H. Bridle, J. A. Dietz and T. R. Morris, JHEP **03** (2014) 093, arXiv:1312.2846.
- [87] G. A. Vilkovisky, in *Quantum Theory Of Gravity*, S. M. Christensen (Ed.), CRC Press, Boca Raton, 1984.
- [88] G. A. Vilkovisky, Nucl. Phys. B **234** (1984) 125.
- [89] B. S. De Witt and C. Molina-Paris, Mod. Phys. Lett. A **13** (1998) 2475, hep-th/9808163.
- [90] L. Parker and D. Toms, *Quantum field theory in curved spacetime*, Cambridge University Press, Cambridge, (2009).
- [91] C. G. Torre, Phys. Rev. D **48** (1993) 2373, gr-qc/9306030.

- [92] K. Groh, Ph.D. thesis, University of Mainz, Germany.
- [93] E. Mottola, J. Math. Phys. **36** (1995) 2470, hep-th/9502109.
- [94] D. F. Litim, Phys. Rev. D **64** (2001) 105007, hep-th/0103195.
- [95] D. F. Litim, Phys. Rev. Lett. **92** (2004) 201301, hep-th/0312114.
- [96] K. Falls, D. F. Litim, K. Nikolakopoulos and C. Rahmede, arXiv:1410.4815.
- [97] M. A. Rubin and C. R. Ordonez, J. Math. Phys. **25** (1984) 2888.
- [98] M. A. Rubin and C. R. Ordonez, J. Math. Phys. **26** (1985) 65.
- [99] I. G. Avramidi, Lect. Notes Phys. M **64** (2000) 1.